



Spectral properties of local gauge invariant composite operators in the $SU(2)$ Yang–Mills–Higgs model

D. Dudal^{1,2,a}, D. M. van Egmond^{3,b} , M. S. Guimarães^{3,c}, L. F. Palhares^{3,d}, G. Peruzzo^{3,e}, S. P. Sorella^{3,f}

¹ Department of Physics, KU Leuven Campus Kortrijk–Kulak, Etienne Sabbelaan 53 bus 7657, 8500 Kortrijk, Belgium

² Department of Physics and Astronomy, Ghent University, Krijgslaan 281-S9, 9000 Ghent, Belgium

³ Departamento de Física Teórica, Instituto de Física, Universidade do Estado do Rio de Janeiro, Rua São Francisco Xavier 524, Maracanã, Rio de Janeiro 20550-013, Brazil

Received: 9 December 2020 / Accepted: 23 February 2021 / Published online: 9 March 2021
© The Author(s) 2021

Abstract The spectral properties of a set of local gauge (BRST) invariant composite operators are investigated in the $SU(2)$ Yang–Mills–Higgs model with a single Higgs field in the fundamental representation, quantized in the 't Hooft R_ξ -gauge. These operators can be thought of as a BRST invariant version of the elementary fields of the theory, the Higgs and gauge fields, with which they share a gauge independent pole mass. The two-point correlation functions of both BRST invariant composite operators and elementary fields, as well as their spectral functions, are investigated at one-loop order. It is shown that the spectral functions of the elementary fields suffer from a strong unphysical dependence from the gauge parameter ξ , and can even exhibit positivity violating behaviour. In contrast, the BRST invariant local operators exhibit a well defined positive spectral density.

1 Introduction

The principle of gauge invariance is the ultimate guideline to formulate quantum field theories of the fundamental interactions as, for example, the electroweak theory [1,2]. In non-Abelian gauge theories, genuine local gauge invariant quantities are associated to composite operators. It is therefore remarkable that the Standard Model is successfully described by employing non-gauge invariant fields as the Higgs and the W and Z elementary fields. Needless to say, the high order calculations of the pole masses and cross sections worked

out by means of these non-gauge invariant fields are in very accurate agreement with the experimental data, see e.g. [3–6] for a few illustrations.

At the theoretical level, the gauge parameter independence of the pole masses of both transverse W and Z bosons as well as of the Higgs field two-point correlation functions are understood by means of the so-called Nielsen identities [7–13], which follow from the Slavnov–Taylor identities encoding the exact BRST symmetry of quantized non-Abelian gauge theories. Nevertheless, as one easily figures out, the direct use of the non-gauge invariant fields displays several limitations, which become more severe in the case of a non-Abelian gauge theory. For instance, in the case of the $U(1)$ Higgs model, the transverse component of the Abelian gauge field A_μ is gauge invariant, so that the two-point correlation function $\mathcal{P}_{\mu\nu}(p)\langle A_\mu(p)A_\nu(-p)\rangle$, where $\mathcal{P}_{\mu\nu}(p) = (\delta_{\mu\nu} - \frac{p_\mu p_\nu}{p^2})$ is the transverse projector, turns out to be independent from the gauge parameter ξ . However, this is no more true in the non-Abelian case, where both Higgs and gauge boson two-point functions, i.e. $\langle h(p)h(-p)\rangle$ and $\mathcal{P}_{\mu\nu}(p)\langle A_\mu^a(p)A_\nu^b(-p)\rangle$, where h stands for the Higgs field and A_μ^a for the gauge boson field, exhibit a strong gauge dependence from ξ . As a consequence, the understanding of the two-point correlation functions of both Higgs field h and gauge vector boson A_μ^a in terms of the Källén–Lehmann (KL) spectral representation is completely jeopardized by an unphysical dependence from the gauge parameter ξ , obscuring a direct interpretation of the above mentioned correlation functions in terms of the elementary excitations of the physical spectrum, namely the Higgs and the vector gauge boson particles. We also note here that from a lattice perspective, it is expected that the spectrum of a gauge (Higgs) theory should be describable in terms of local gauge invariant operator correlation functions, with concrete physical information hiding in the various (positive and gauge invariant) spec-

^a e-mail: david.dudal@kuleuven.be

^b e-mail: duifjemaria@gmail.com (corresponding author)

^c e-mail: msguimaraes@uerj.br

^d e-mail: leticia.palhares@uerj.br

^e e-mail: gperuzzofisica@gmail.com

^f e-mail: silvio.sorella@gmail.com

tral functions, not only pole masses, decay widths, but also transport coefficients at finite temperature etc. Clearly, such information will not correctly be encoded in gauge variant, non-positive spectral functions.

Within this perspective, the use of manifest gauge invariant variables to describe the Higgs and the vector gauge bosons is certainly very welcome. This endeavour was first proposed by 't Hooft in [1], and later on formalized by Fröhlich, Morchio and Strocchi (FMS) in [14, 15]. These authors were able to build, out of the elementary fields, a set of local composite gauge invariant operators $\{\tilde{\mathcal{O}}(x)\}$ which, when expanded around the value $\Phi = \text{constant}$ which minimizes the Higgs potential present in the starting classical action, give rise to two-point functions which enjoy the important property of reproducing, at the tree level, the two-point correlation functions of the elementary fields $\{\varphi\} = (A_\mu^a, h)$, namely

$$\langle \tilde{\mathcal{O}}(x)\tilde{\mathcal{O}}(y) \rangle \sim \langle \varphi(x)\varphi(y) \rangle_{\text{tree}} + \dots, \tag{1}$$

where \dots denote the higher order loop corrections which will be the main subject of the present work. Equation (1) shows in a very simple and intuitive way the relevance of the composite operators $\{\tilde{\mathcal{O}}(x)\}$ in order to provide a description of the gauge vector bosons and of the Higgs particle within a fully gauge invariant environment, see also the recent works [16–19] where, amongst other things, a lattice formulation has been proposed. Certain aspects of a gauge invariant version of the Higgs phenomenon were also covered in [20, 21], albeit whilst assuming the “frozen” radial limit, $\varphi^\dagger\varphi = \text{fixed}$, corresponding to a Higgs coupling $\lambda \rightarrow \infty$, a formal limit hampering explicit computations in the continuum. Further attempts towards a gauge-invariant formulation of the Higgs phenomenon can be found in [22].

In two earlier works [23, 24], we have laid the ground for the study of the spectral properties of the gauge (BRST) invariant local composite operators $\{\tilde{\mathcal{O}}(x)\}$ in the FMS framework. In [24], we have made the first analytic one-loop calculations of these BRST invariant operators in the simpler $U(1)$ Higgs model quantized in the R_ξ -gauge. In particular, we have worked out the one-loop corrections to the two-point functions in Eq. (1) corresponding to the Higgs and Abelian gauge fields and we have shown that they have the same gauge independent pole masses of the corresponding elementary two-point correlation functions. In addition, we have explicitly shown that the correlation functions of the composite operators display a well defined positive and gauge independent Källén–Lehmann spectral representation, a feature not shared by the two-point correlation functions of the elementary fields which, as in the explicit case of the Higgs field, i.e. $\langle h(p)h(-p) \rangle$, display an unphysical dependence from the gauge parameter ξ , becoming even negative depending on the value of ξ . Moreover, in [25], the renormal-

ization properties of these composite operators were scrutinized using the algebraic renormalization approach.

The aim of the present work is that of extending the techniques of [23, 24] to the more complex case of $SU(2)$ Higgs model with a single Higgs field in the fundamental representation. As we shall see, besides the exact BRST invariance, the quantized theory exhibits a global $SU(2)$ symmetry commonly referred to as the *custodial symmetry*. Moreover, the local composite BRST invariant operators corresponding to the gauge bosons transform as a triplet under the custodial symmetry, a property which will imply useful relations for their two-point correlation functions.

The present work is organized as follows. In Sect. 2, we give a review of the $SU(2)$ Yang–Mills–Higgs model with a single Higgs field in the fundamental representation, of the gauge fixing procedure and its ensuing BRST invariance. In Sect. 3 we calculate the two-point correlation functions of the elementary fields up to one-loop order. In Sect. 4, we define the BRST invariant local composite operators $(\mathcal{O}(x), R_\mu^a(x))$ corresponding to the BRST invariant extension of (h, A_μ^a) and calculate their one-loop correlation functions. In Sect. 5, we discuss the spectral properties of both elementary and composite operators.

In order to give a more general idea of the behavior of the spectral functions, we shall be using two sets of parameters which we shall refer as to Region I and Region II. To some extent, Region II can be associated to the perturbative weak coupling regime, while in Region I we keep the gauge coupling a little bit larger, while decreasing the vev (vacuum expectation value) of the Higgs field. Section 6 is devoted to our conclusion and outlook. The technical details are all collected in the Appendices.

2 The action and its symmetries

The Yang–Mills action with a single Higgs field in the fundamental representation is given by

$$\begin{aligned} S_0 &= \int d^4x \left\{ \frac{1}{4} F_{\mu\nu}^a F_{\mu\nu}^a + (D_\mu^{ij} \Phi^{\dagger j})(D_\mu^{ik} \Phi^k) \right. \\ &\quad \left. + \frac{\lambda}{2} \left(\Phi^{\dagger i} \Phi^i - \frac{1}{2} v^2 \right)^2 \right\} \\ &= S_{\text{YM}} + S_{\text{Higgs}} \end{aligned} \tag{2}$$

with

$$F_{\mu\nu} = \partial_\mu A_\nu^a - \partial_\nu A_\mu^a + g\epsilon^{abc} A_\mu^b A_\nu^c \tag{3}$$

and

$$D_\mu^{ij} \Phi^j = \partial_\mu \Phi^i - \frac{i}{2} g(\tau^a)^{ij} A_\mu^a \Phi^j,$$

$$(D_{\mu}^{ij} \Phi^j)^{\dagger} = \partial_{\mu} \Phi^{i\dagger} + \frac{i}{2} g \Phi^{j\dagger} (\tau^a)^{ji} A_{\mu}^a, \tag{4}$$

with the Pauli matrices τ^a ($a = 1, 2, 3$) and the Levi-Civita tensor ϵ^{abc} referring to the gauge symmetry group $SU(2)$. The scalar complex field $\Phi^i(x)$ is in the fundamental representation of $SU(2)$, i.e. $i, j = 1, 2$. Thus, Φ is an $SU(2)$ -doublet of complex scalar fields that can be written as

$$\Phi = \frac{1}{\sqrt{2}} \begin{pmatrix} \phi^+ \\ \phi^0 \end{pmatrix} = \frac{1}{\sqrt{2}} \begin{pmatrix} \phi_1 + i\phi_2 \\ \phi_3 + i\phi_4 \end{pmatrix}. \tag{5}$$

We will work in Euclidean space-time throughout this paper.

The configuration which minimizes the Higgs potential in the expression (2) is

$$\langle \Phi \rangle = \frac{1}{\sqrt{2}} \begin{pmatrix} v \\ 0 \end{pmatrix} \tag{6}$$

and we write down $\Phi(x)$ as an expansion around the configuration (6), so that

$$\Phi = \frac{1}{\sqrt{2}} \begin{pmatrix} v + h + i\rho_3 \\ i\rho_1 - \rho_2 \end{pmatrix}, \tag{7}$$

where h is the Higgs field and ρ^a , $a = 1, 2, 3$, the would-be Goldstone bosons. We can use the matrix notation¹:

$$\Phi = \frac{1}{\sqrt{2}} ((v + h)\mathbf{1} + i\rho^a \tau^a) \cdot \begin{pmatrix} 1 \\ 0 \end{pmatrix}, \tag{8}$$

so that the second term in Eq. (2) becomes

$$\begin{aligned} (D_{\mu}^{ij} \Phi^j)^{\dagger} D_{\mu}^{ik} \Phi^k &= \frac{1}{2} (1, 0) \cdot \left[\partial_{\mu} h \cdot \mathbf{1} - i\partial_{\mu} \rho^a \tau^a \right. \\ &\quad \left. + \frac{ig}{2} \tau^a A_{\mu}^a ((v + h)\mathbf{1} - i\rho^b \tau^b) \right] \\ &\quad \times \left[\partial_{\mu} h \cdot \mathbf{1} + i\partial_{\mu} \rho^c \tau^c - \frac{ig}{2} ((v + h)\mathbf{1} - i\rho^d \tau^d) \tau^c A_{\mu}^c \right] \cdot \begin{pmatrix} 1 \\ 0 \end{pmatrix} \\ &= \tilde{\mathcal{L}}_0 + \tilde{\mathcal{L}}_1 + \tilde{\mathcal{L}}_2, \end{aligned} \tag{9, 10}$$

with $\tilde{\mathcal{L}}_i$ the i th term in powers of A_{μ} :

$$\begin{aligned} \tilde{\mathcal{L}}_0 &= \frac{1}{2} \left((\partial_{\mu} h)^2 + \partial_{\mu} \rho^a \partial_{\mu} \rho^a \right), \\ \tilde{\mathcal{L}}_1 &= -\frac{1}{2} \left\{ g v A_{\mu}^a \partial_{\mu} \rho^a - g A_{\mu}^a \rho^a \partial_{\mu} h \right. \\ &\quad \left. + g A_{\mu}^a (\partial_{\mu} \rho^a) h + g \epsilon^{abc} \partial_{\mu} \rho^a \rho^b A_{\mu}^c \right\}, \\ \tilde{\mathcal{L}}_2 &= \frac{g^2}{8} A_{\mu}^a A_{\mu}^a \left[(v + h)^2 + \rho^b \rho^b \right], \end{aligned} \tag{11}$$

and we have the full action

$$S_0 = \int d^4x \frac{1}{2} \left\{ \frac{1}{2} F_{\mu\nu}^a F_{\mu\nu}^a + \frac{1}{4} v^2 g^2 A_{\mu}^a A_{\mu}^a + (\partial_{\mu} h)^2 \right.$$

$$\begin{aligned} &\quad \left. + \partial_{\mu} \rho^a \partial_{\mu} \rho^a - g v A_{\mu}^a \partial_{\mu} \rho^a \right. \\ &\quad \left. + g A_{\mu}^a \rho^a \partial_{\mu} h - g A_{\mu}^a (\partial_{\mu} \rho^a) h \right. \\ &\quad \left. - g \epsilon^{abc} \partial_{\mu} \rho^a \rho^b A_{\mu}^c + \frac{g^2}{4} A_{\mu}^a A_{\mu}^a \left[2vh + h^2 + \rho^b \rho^b \right] \right. \\ &\quad \left. + \lambda v^2 h^2 + \lambda v h (h^2 + \rho^a \rho^a) \right. \\ &\quad \left. + \frac{\lambda}{4} (h^2 + \rho^a \rho^a)^2 \right\}. \end{aligned} \tag{12}$$

One sees that both gauge field A_{μ}^a and Higgs field h have acquired a mass given, respectively, by

$$m^2 = \frac{1}{4} g^2 v^2, \quad m_h^2 = \lambda v^2. \tag{13}$$

2.1 Gauge fixing and BRST symmetry

The action (2) is invariant under the local ω -parametrized gauge transformations

$$\delta A_{\mu}^a = -D_{\mu}^{ab} \omega^b, \quad \delta \Phi = -\frac{ig}{2} \omega^a \tau^a \Phi, \quad \delta \Phi^{\dagger} = \frac{ig}{2} \omega^a \Phi^{\dagger} \tau^a, \tag{14}$$

which, when written in terms of the fields (h, ρ^a) , become

$$\delta h = \frac{g}{2} \omega^a \rho^a, \quad \delta \rho^a = -\frac{g}{2} (\omega^a (v + h)\mathbf{1} - \epsilon^{abc} \omega^b \rho^c). \tag{15}$$

As done in the $U(1)$ case [23, 24], we shall be using the R_{ξ} -gauge. We add thus need the gauge fixing term

$$\begin{aligned} S_{\text{gf}} &= s \int d^4x \left\{ -i \frac{\xi}{2} \bar{c}^a b^a + \bar{c}^a (\partial_{\mu} A_{\mu}^a - \xi m \rho^a) \right\} \\ &= \frac{1}{2} \int d^4x \left\{ \xi b^a b^a \right. \\ &\quad \left. + 2i b^a \partial_{\mu} A_{\mu}^a + 2\bar{c}^a \partial_{\mu} D_{\mu}^{ab} c^b - 2i \xi m b^a \rho^a \right. \\ &\quad \left. - 2\xi \bar{c}^a m c^a - g \xi \bar{c}^a m h c^a - \xi g \epsilon^{abc} \bar{c}^a c^b \rho^c \right\}, \end{aligned} \tag{16}$$

so that the gauge fixed action $S_{\text{full}} = S_0 + S_{\text{gf}}$, namely

$$\begin{aligned} S_{\text{full}} &= \int d^4x \frac{1}{2} \left\{ \frac{1}{2} F_{\mu\nu}^a F_{\mu\nu}^a + \frac{1}{4} v^2 g^2 A_{\mu}^a A_{\mu}^a \right. \\ &\quad \left. + (\partial_{\mu} h)^2 + \partial_{\mu} \rho^a \partial_{\mu} \rho^a - g v A_{\mu}^a \partial_{\mu} \rho^a \right. \\ &\quad \left. + g A_{\mu}^a \rho^a \partial_{\mu} h - g A_{\mu}^a (\partial_{\mu} \rho^a) h \right. \\ &\quad \left. - g \epsilon^{abc} \partial_{\mu} \rho^a \rho^b A_{\mu}^c \right. \\ &\quad \left. + \frac{g^2}{4} A_{\mu}^a A_{\mu}^a \left[2vh + h^2 + \rho^b \rho^b \right] + \lambda v^2 h^2 \right. \\ &\quad \left. + \lambda v h (h^2 + \rho^a \rho^a) + \frac{\lambda}{4} (h^2 + \rho^a \rho^a)^2 + \xi b^a b^a \right. \\ &\quad \left. + 2i b^a \partial_{\mu} A_{\mu}^a + 2\bar{c}^a \partial_{\mu} D_{\mu}^{ab} c^b - 2i \xi m b^a \rho^a \right. \\ &\quad \left. - 2\xi \bar{c}^a m c^a - g \xi \bar{c}^a m h c^a \right. \\ &\quad \left. - \xi g \epsilon^{abc} \bar{c}^a c^b \rho^c \right\} \end{aligned} \tag{17}$$

¹ This is of course possible thanks to the fact that Φ counts 3 Goldstone modes and that $SU(2)$ has three generators. This “numerology” is essentially what leads to a large custodial symmetry in the $SU(2)$ case.

turns out to be left invariant by the BRST transformations

$$sA_\mu^a = -D_\mu^{ab} c^b, \quad sh = \frac{g}{2} c^a \rho^a,$$

$$s\rho^a = -\frac{g}{2} (c^a (v + h) - \epsilon^{abc} c^b \rho^c)$$

$$sc^a = \frac{1}{2} g \epsilon^{abc} c^b c^c, \quad s\bar{c}^a = ib^a, \quad sb^a = 0, \tag{18}$$

$$sS_{\text{full}} = 0. \tag{19}$$

The Feynman rules for the full action (17) are given in Appendix A. Notice that in the R_ξ -gauge the tree-level propagator $\langle A_\mu^a(x) \rho^a(y) \rangle$ vanishes, a well-known feature of this gauge choice [2]. We will assume that $\xi \geq 0$ to avoid tachyon poles in elementary propagators, see Eq. (A1).

2.2 Custodial symmetry

As already mentioned, apart from the BRST symmetry, there is an extra global symmetry, which we shall refer to as the custodial symmetry:

$$\delta A_\mu^a = \epsilon^{abc} \beta^b A_\mu^c,$$

$$\delta \rho^a = \epsilon^{abc} \beta^b \rho^c,$$

$$\delta \bar{c}^a = \epsilon^{abc} \beta^b \bar{c}^c,$$

$$\delta c^a = \epsilon^{abc} \beta^b c^c,$$

$$\delta b^a = \epsilon^{abc} \beta^b b^c,$$

$$\delta h = 0, \tag{20}$$

where β^a is a constant parameter, $\partial_\mu \beta^a = 0$,

$$\delta S_{\text{full}} = 0. \tag{21}$$

One notices that all fields carrying the index $a = 1, 2, 3$, i.e. $(A_\mu^a, b^a, c^a, \bar{c}^a, \rho^a)$, undergo a global transformation in the adjoint representation of $SU(2)$. The origin of this symmetry is an $SU(2)_{\text{gauge}} \times SU(2)_{\text{global}}$ symmetry of the action in the unbroken phase, see Appendix B. The exception is the Higgs field h , which is left invariant, i.e. it is a singlet. As we shall see in the following, this additional global symmetry will provide useful relationships for the two-point correlation functions of the BRST invariant composite operators.

3 One-loop evaluation of the correlation function of the elementary fields

For the elementary fields $h(x)$ and A_μ^a , the correlation functions are calculated up to first loop order in Appendices C0a and C0b. In what follows, we will always spell out again the momentum-dependent logarithms and explicit Feynman parameter dependence, that is, we will in the eventual correlation functions replace again the notational shorthands introduced in Eq. (C1). The Feynman parameter integration itself

was handled via (F1). We have used the explicit expression (F1) to numerically construct our spectral function plots (see later). More about that integral (F1) can be found in [26, 27].

For the Higgs field, for the propagator we get

$$\langle h(p)h(-p) \rangle = \frac{1}{p^2 + m_h^2} + \frac{1}{(p^2 + m_h^2)^2} \Pi_{hh}(p^2) + \mathcal{O}(\hbar^2), \tag{22}$$

with $\Pi_{hh}(p^2)$ the one-loop correction to the self-energy calculated in Appendix C0a. For $d = 4$, this correction is divergent. Employing the procedure of dimensional regularization, i.e. setting $d = 4 - \epsilon$, the divergent part for $\Pi_{hh}(p^2)$ is given by:

$$\Pi_{hh,\text{div}}(p^2) = \frac{g^2 \left(\frac{3m_h^4}{m^2} - 3\xi m_h^2 - 3\xi p^2 + 9p^2 \right)}{32\pi^2 \epsilon}, \tag{23}$$

which, following the $\overline{\text{MS}}$ -scheme, is re-absorbed by the introduction of suitable local counterterms. We remain thus with the finite part of the Higgs self-energy

$$\begin{aligned} \Pi_{hh}(p^2) = & \frac{3g^2}{8(4\pi)^2} \int_0^1 dx \left\{ 2\xi \left(m_h^2 + p^2 \right) \ln \left(\frac{m^2 \xi}{\mu^2} \right) \right. \\ & - 2\xi m_h^2 + 2 \left(6m^2 - p^2 \right) \ln \left(\frac{m^2}{\mu^2} \right) \\ & - \left(12m^2 + \frac{p^4}{m^2} + 4p^2 \right) \ln \left(\frac{m^2 + p^2(1-x)x}{\mu^2} \right) \\ & + \left(\frac{p^4}{m^2} - \frac{m_h^4}{m^2} \right) \ln \left(\frac{m^2 \xi + p^2(1-x)x}{\mu^2} \right) \\ & - 12m^2 - 2\xi p^2 + 2p^2 \\ & - \frac{m_h^4}{m^2} \left(-2 \ln \left(\frac{m_h^2}{\mu^2} \right) \right. \\ & \left. \left. + 3 \ln \left(\frac{m_h^2 + p^2(1-x)x}{\mu^2} \right) + 2 \right) \right\}. \tag{24} \end{aligned}$$

Before trying to resum the self-energy $\Pi_{hh}(p^2)$, we notice that this resummation is tacitly assuming that the second term in (22) is much smaller than the first term. However, we see that Eq. (22) contains terms of the order of $\frac{p^4}{(p^2+m_h^2)^2} \ln \left(\frac{m^2+p^2(1-x)x}{\mu^2} \right)$ which cannot be resummed for big values of p^2 .

Indeed, if one proceeds naively and include these large contributions into a resummation, spurious tachyon poles will be induced in the correlator, analogous as in the earlier investigated $U(1)$ case in [24]. The need for care in resumming these contributions was also strengthened and worked out in great detail in [28].

We therefore proceed as in [23,24] and use the identity

$$p^4 = (p^2 + m_h^2)^2 - m_h^4 - 2p^2 m_h^2 \tag{25}$$

to rewrite

$$\begin{aligned} & \frac{p^4}{(p^2 + m_h^2)^2} \ln \frac{p^2 x(1-x) + m^2}{\mu^2} \\ &= \ln \frac{p^2 x(1-x) + m^2}{\mu^2} \\ & \quad - \frac{(m_h^4 + 2p^2 m_h^2)}{(p^2 + m_h^2)^2} \ln \frac{p^2 x(1-x) + m^2}{\mu^2}. \end{aligned} \tag{26}$$

The term which has been underlined in Eq. (26) can be safely resummed, as it decays fast enough for large values of p^2 . We thence rewrite

$$\frac{\Pi_{hh}(p^2)}{(p^2 + m_h^2)^2} = \frac{\hat{\Pi}_{hh}(p^2)}{(p^2 + m_h^2)^2} + C_{hh}(p^2), \tag{27}$$

with

$$\begin{aligned} \hat{\Pi}_{hh}(p^2) = & \frac{3g^2}{8(4\pi)^2} \int_0^1 dx \left\{ 2\xi (m_h^2 + p^2) \ln \left(\frac{m^2 \xi}{\mu^2} \right) \right. \\ & - 2\xi m_h^2 + 2(6m^2 - p^2) \ln \left(\frac{m^2}{\mu^2} \right) \\ & - (12m^2 - \frac{m_h^4 + 2p^2 m_h^2}{m^2} + 4p^2) \\ & \times \ln \left(\frac{m^2 + p^2(1-x)x}{\mu^2} \right) \\ & - \frac{(2m_h^4 + 2p^2 m_h^2)}{m^2} \ln \left(\frac{m^2 \xi + p^2(1-x)x}{\mu^2} \right) \\ & - 12m^2 - 2\xi p^2 + 2p^2 - \frac{m_h^4}{m^2} \left(-2 \ln \left(\frac{m_h^2}{\mu^2} \right) \right. \\ & \left. \left. + 3 \ln \left(\frac{m_h^2 + p^2(1-x)x}{\mu^2} \right) + 2 \right) \right\} \end{aligned} \tag{28}$$

and

$$\begin{aligned} C_{hh}(p^2) = & -\frac{3g^2}{8m^2(4\pi)^2} \int_0^1 dx \\ & \times \left(\ln \frac{p^2 x(1-x) + m^2}{\mu^2} - \ln \frac{p^2 x(1-x) + \xi m^2}{\mu^2} \right). \end{aligned} \tag{29}$$

Thus, for the one-loop Higgs propagator, we get

$$\langle h(p)h(-p) \rangle = \frac{1}{p^2 + m_h^2 - \hat{\Pi}_{hh}(p^2)} + C_{hh}(p^2) + \mathcal{O}(\hbar^2). \tag{30}$$

For the gauge field, we split the two-point function into transverse and longitudinal parts in the usual way

$$\langle A_\mu^a(p)A_\nu^b(-p) \rangle = \left[D_{AA}^T(p^2)\mathcal{P}_{\mu\nu}(p) + D_{AA}^L(p^2)\mathcal{L}_{\mu\nu}(p) \right] \delta^{ab}, \tag{31}$$

where we have introduced the transverse and longitudinal projectors, given respectively by

$$\mathcal{P}_{\mu\nu}(p) = \delta_{\mu\nu} - \frac{p_\mu p_\nu}{p^2}, \quad \mathcal{L}_{\mu\nu}(p) = \frac{p_\mu p_\nu}{p^2}. \tag{32}$$

We find

$$D_{AA}^T(p^2) = \frac{1}{p^2 + m^2} + \frac{1}{(p^2 + m^2)^2} \Pi_{AA^T}(p^2) + \mathcal{O}(\hbar^2), \tag{33}$$

with $\Pi_{AA^T}(p^2)$ the one-loop correction to the self-energy calculated in Appendix C0b. For $d = 4 - \epsilon$, following the procedure of dimensional regularization, we find that the divergent part for $\Pi_{AA^T}(p^2)$ is given by:

$$\begin{aligned} \Pi_{AA^T, \text{div}}(p^2) = & \frac{g^2}{\pi^2 \epsilon} \left(-\frac{9m^4}{16m_h^2} \right. \\ & \left. - \frac{3m_h^2}{32} - \frac{m^2 \xi}{8} - \frac{3m^2}{32} - \frac{\xi p^2}{8} + \frac{25p^2}{48} \right), \end{aligned} \tag{34}$$

and these terms can be, following the $\overline{\text{MS}}$ -scheme, absorbed by means of appropriate counterterms. We remain with the finite part of the self-energy²

$$\begin{aligned} \Pi_{AA^T}(p^2) = & -\frac{g^2}{36(4\pi)^2 m^4 p^2 m_h^2} \int_0^1 dx \left\{ -27m^4 p^2 m_h^4 \ln \left(\frac{m_h^2}{\mu^2} \right) \right. \\ & - 27m^6 \xi p^2 m_h^2 \ln \left(\frac{m^2 \xi}{\mu^2} \right) \\ & + 3m^4 m_h^4 (m_h^2 - m^2 + 2p^2) \ln \left(\frac{m_h^2}{\mu^2} \right) \\ & + 27m^4 p^2 m_h^2 (m_h^2 + m^2 \xi) \\ & - 3m^4 \xi m_h^2 (2m^4 (\xi - 1) + m^2 (4\xi + 7)) p^2 \\ & + 2(\xi + 9) p^4 \ln \left(\frac{m^2 \xi}{\mu^2} \right) \\ & + 3m^4 \ln \left(\frac{m^2}{\mu^2} \right) (-m^2 m_h^4 + m_h^2 (m^4 (2\xi - 1) \\ & + m^2 (4\xi + 45) p^2 + 2(\xi + 9) p^4) - 54m^4 p^2) \\ & + m^4 (6m^2 m_h^4 + m_h^2 (3m^4 (2(\xi - 2)\xi + 1) \\ & \left. + 3m^2 (\xi - 1)(4\xi - 1) p^2 + 2(3\xi (\xi + 4) - 17) p^4) \right) \end{aligned}$$

² For notational simplicity, we will call this finite part Π_{AA^T} again. We will follow this notational convention as well for later correlation functions that we will encounter.

$$\begin{aligned}
 & -3m_h^6 + 54m^4 p^2) - 3m_h^2 \left[m^4 (2p^2 (m_h^2 - 5m^2) \right. \\
 & + (m_h^2 - m^2)^2 + p^4) \\
 & \times \ln \left(\frac{p^2(1-x)x + m_h^2(1-x) + m^2x}{\mu^2} \right) \\
 & -2(m^2 + p^2)^2 (m^4(\xi - 1)^2 + 2m^2(\xi - 5)p^2 + p^4) \\
 & \times \ln \left(\frac{p^2(1-x)x + \xi m^2(1-x) + m^2x}{\mu^2} \right) \\
 & + p^2 (p^4 - m^4) (4m^2\xi + p^2) \\
 & \times \ln \left(\frac{p^2(1-x)x + \xi m^2}{\mu^2} \right) \\
 & + p^2 (4m^2 + p^2) (12m^4 - 20m^2 p^2 + p^4) \\
 & \left. \times \ln \left(\frac{p^2(1-x)x + m^2}{\mu^2} \right) \right] \}. \tag{35}
 \end{aligned}$$

We see that (33) contains again terms of the order $\frac{p^4}{(p^2+m^2)^2} \ln \left(\frac{m^2+p^2(1-x)x}{\mu^2} \right)$ and $\frac{p^6}{(p^2+m^2)^2} \ln \left(\frac{m^2+p^2(1-x)x}{\mu^2} \right)$, which cannot be resummed for big values of p^2 . We use

$$\begin{aligned}
 & \frac{p^4}{(p^2 + m^2)^2} \ln \frac{p^2x(1-x) + m^2}{\mu^2} \\
 & = \ln \frac{p^2x(1-x) + m^2}{\mu^2} \\
 & \quad - \frac{(m^4 + 2p^2m^2)}{(p^2 + m^2)^2} \ln \frac{p^2x(1-x) + m^2}{\mu^2} \tag{36}
 \end{aligned}$$

and

$$\begin{aligned}
 & \frac{p^6}{(p^2 + m^2)^2} \ln \frac{p^2x(1-x) + m^2}{\mu^2} \\
 & = (p^2 - 2m^2) \ln \frac{p^2x(1-x) + m^2}{\mu^2} \\
 & \quad + \frac{2m^6 + 3p^2m^4}{(p^2 + m^2)^2} \ln \frac{p^2x(1-x) + m^2}{\mu^2}. \tag{37}
 \end{aligned}$$

The underlined terms in (36) and (37) can be safely resummed. We rewrite

$$\frac{\Pi_{AA^T}(p^2)}{(p^2 + m^2)^2} = \frac{\hat{\Pi}_{AA^T}(p^2)}{(p^2 + m_h^2)^2} + C_{AA^T}(p^2), \tag{38}$$

with

$$\begin{aligned}
 \hat{\Pi}_{AA^T}(p^2) & = -\frac{g^2}{36(4\pi)^2 m^4 p^2 m_h^2} \int_0^1 dx \\
 & \times \left\{ -27m^4 p^2 m_h^4 \ln \left(\frac{m_h^2}{\mu^2} \right) - 27m^6 \xi p^2 m_h^2 \ln \left(\frac{m^2 \xi}{\mu^2} \right) \right. \\
 & \left. + 3m^4 m_h^4 (m_h^2 - m^2 + 2p^2) \ln \left(\frac{m_h^2}{\mu^2} \right) \right.
 \end{aligned}$$

$$\begin{aligned}
 & + 27m^4 p^2 m_h^2 (m_h^2 + m^2 \xi) \\
 & - 3m^4 \xi m_h^2 (2m^4 (\xi - 1) + m^2 (4\xi + 7) p^2) \\
 & + 2(\xi + 9) p^4 \ln \left(\frac{m^2 \xi}{\mu^2} \right) \\
 & + 3m^4 (-m^2 m_h^4 + m_h^2 (m^4 (2\xi - 1) \\
 & + m^2 (4\xi + 45) p^2 + 2(\xi + 9) p^4) \\
 & - 54m^4 p^2) \ln \left(\frac{m^2}{\mu^2} \right) \\
 & + m^4 (6m^2 m_h^4 + m_h^2 (3m^4 (2(\xi - 2)\xi + 1) \\
 & + 3m^2 (\xi - 1) (4\xi - 1) p^2 \\
 & + 2(3\xi (\xi + 4) - 17) p^4) - 3m_h^6 + 54m^4 p^2) \\
 & - 3m_h^2 \left[m^4 (2p^2 (m_h^2 - 5m^2) + (m_h^2 - m^2)^2 + p^4) \right. \\
 & \times \ln \left(\frac{p^2(1-x)x + (1-x)m_h^2 + m^2x}{\mu^2} \right) \\
 & - 2m^4 (\xi - 1)^2 (m^2 + p^2)^2 \\
 & \times \ln \left(\frac{p^2(1-x)x + \xi m^2(1-x) + m^2x}{\mu^2} \right) \\
 & + (-2m^4 (4\xi - 1) p^2 (m^2 + p^2)) \\
 & \times \ln \left(\frac{p^2(1-x)x + \xi m^2}{\mu^2} \right) \\
 & \left. \left. + (66m^6 p^2 - 33m^4 p^4) \ln \left(\frac{p^2(1-x)x + m^2}{\mu^2} \right) \right] \right\}. \tag{39}
 \end{aligned}$$

and

$$\begin{aligned}
 C_{AA^T}(p^2) & = \frac{g^2}{12(4\pi)^2 m^4} \int_0^1 dx \left\{ (-4m^2 (\xi - 5) - 2p^2) \right. \\
 & \times \ln \left(\frac{p^2(1-x)x + \xi m^2(1-x) + m^2x}{\mu^2} \right) \\
 & + (4\xi m^2 + p^2 - 2m^2) \ln \left(\frac{p^2(1-x)x + \xi m^2}{\mu^2} \right) \\
 & \left. + (-18m^2 + p^2) \ln \left(\frac{p^2(1-x)x + m^2}{\mu^2} \right) \right\}. \tag{40}
 \end{aligned}$$

Finally

$$D_{AA}^T(p^2) = \left(\frac{1}{p^2 + m^2 - \hat{\Pi}_{AA^T}(p^2)} + C_{AA^T}(p^2) \right) + \mathcal{O}(\hbar^2). \tag{41}$$

4 One-loop evaluation of the correlation function of the local BRST invariant composite operators

4.1 Correlation function of the scalar BRST invariant composite operator $O(x)$

The gauge and BRST invariant local scalar composite operator $O(x)$ is given by

$$O(x) = \Phi^\dagger \Phi - \frac{v^2}{2}, \quad s O(x) = 0, \tag{42}$$

which, after using the expansion (8), becomes

$$\begin{aligned} O(x) &= \frac{1}{2} \left[(1 \ 0) ((v+h)\mathbf{1} - i\rho^a \tau^a) ((v+h)\mathbf{1} \right. \\ &\quad \left. + i\rho^b \tau^b) \begin{pmatrix} 1 \\ 0 \end{pmatrix} \right] - \frac{v^2}{2} \\ &= \frac{1}{2} (h^2(x) + 2vh(x) + \rho^a(x)\rho^a(x)). \end{aligned} \tag{43}$$

Notice that the operator $O(x)$ does not depend on the FP ghost field. Therefore,

$$\begin{aligned} \langle O(x)O(y) \rangle &= v^2 \langle h(x)h(y) \rangle \\ &\quad + v \langle h(x)\rho^b(y)\rho^b(y) \rangle + v \langle h(x)h(y)^2 \rangle \\ &\quad + \frac{1}{4} \langle h(x)^2 \rho^b(y)\rho^b(y) \rangle + \frac{1}{4} \langle h(x)^2 h(y)^2 \rangle \\ &\quad + \frac{1}{4} \langle \rho^a(x)\rho^a(x)\rho^b(y)\rho^b(y) \rangle. \end{aligned} \tag{44}$$

Looking at the tree level expression of Eq. (44), one easily obtains

$$\langle O(p)O(-p) \rangle_{\text{tree}} = v^2 \langle h(p)h(-p) \rangle_{\text{tree}} = v^2 \frac{1}{p^2 + m_h^2}, \tag{45}$$

showing that the BRST invariant scalar operator $O(x)$ is directly linked to the Higgs propagator.

Concerning now the one-loop calculation of expression (44), after evaluating each term, see Appendix D for details, we find that the two-point correlation function of the scalar composite operator $O(x)$ develops a geometric series in the same way as the elementary field $h(x)$. This allows us to make a resummed approximation. Using dimensional regularization in the $\overline{\text{MS}}$ -scheme, we find that, in the R_ξ -gauge

$$\begin{aligned} \langle O(p)O(-p) \rangle(p^2) &= \frac{v^2}{p^2 + m_h^2} \\ &\quad + \frac{v^2}{(p^2 + m_h^2)^2} \Pi_{OO}(p^2) + \mathcal{O}(\hbar^2), \end{aligned} \tag{46}$$

with $\Pi_{OO}(p^2)$ the one-loop correction calculated in Appendix D. Following the procedure of dimensional regularization for

$d = 4 - \epsilon$, we find that the divergent part of the one-loop correction is given by

$$\begin{aligned} \Pi_{OO,\text{div}}^{-1} &= \frac{1}{4v^2\pi^2\epsilon} \left(\frac{9g^4 p^2 v^2}{16\lambda} + \frac{9g^4 v^4}{16} \right. \\ &\quad \left. + \frac{9}{8} g^2 p^2 v^2 + p^4 + \frac{1}{2} \lambda p^2 v^2 + \lambda^2 v^4 \right), \end{aligned} \tag{47}$$

which can be accounted for by appropriate counterterms, following the $\overline{\text{MS}}$ -scheme renormalization procedure. A full renormalization analysis will be presented elsewhere. Notice that expression (47), when multiplied again with the factored-out v^2 of Eq. (46), is a polynomial in p^2, v^2 , in full accordance with power counting renormalizability.

We remain with the finite part, given by

$$\begin{aligned} \Pi_{OO}(p^2) &= \frac{1}{32v^2\pi^2 m_h^2} \int_0^1 dx \left\{ -24m_h^2 m^4 \right. \\ &\quad - 6m^2 p^2 (m_h^2 + 6m^2) \ln \left(\frac{m^2}{\mu^2} \right) \\ &\quad - m_h^2 (p^2 - 2m_h^2)^2 \ln \left(\frac{m_h^2 + p^2 x(1-x)}{\mu^2} \right) \\ &\quad - 3m_h^2 (12m^4 + 4m^2 p^2 + p^4) \ln \left(\frac{m^2 + p^2 x(1-x)}{\mu^2} \right) \\ &\quad \left. + 6p^2 (m_h^4 + m_h^2 m^2 + 2m^4) - 6m_h^4 p^2 \ln \left(\frac{m_h^2}{\mu^2} \right) \right\}. \end{aligned} \tag{48}$$

Since (46) contains terms of the order of $\frac{p^4}{(p^2+m^2)^2} \ln(p^2)$, we follow the steps (36)–(38) to find the resummed correlation function in the one-loop approximation

$$G_{OO}(p^2) = \frac{v^2}{p^2 + m_h^2 - \hat{\Pi}_{OO}(p^2)} + C_{OO}(p^2) \tag{49}$$

with

$$\begin{aligned} \hat{\Pi}_{OO}(p^2) &= \frac{1}{32v^2\pi^2 m_h^2} \int_0^1 dx \left\{ -24m_h^2 m^4 \right. \\ &\quad - 6m^2 p^2 (m_h^2 + 6m^2) \ln \left(\frac{m^2}{\mu^2} \right) \\ &\quad - m_h^2 (3m_h^4 - 6m_h^2 p^2) \ln \left(\frac{m_h^2 + p^2 x(1-x)}{\mu^2} \right) \\ &\quad - 3m_h^2 (12m^4 + 4m^2 p^2 - m_h^4 - 2p^2 m_h^2) \\ &\quad \times \ln \left(\frac{m^2 + p^2 x(1-x)}{\mu^2} \right) \\ &\quad \left. + 6p^2 (m_h^4 + m_h^2 m^2 + 2m^4) - 6m_h^4 p^2 \ln \left(\frac{m_h^2}{\mu^2} \right) \right\} \end{aligned} \tag{50}$$

and

$$C_{OO}(p^2) = -\frac{1}{32\pi^2} \int_0^1 dx \left\{ \ln \left(\frac{m_h^2 + p^2 x(1-x)}{\mu^2} \right) + 3 \ln \left(\frac{m^2 + p^2 x(1-x)}{\mu^2} \right) \right\}. \tag{51}$$

Expressions (49) and (51) show that, as expected, and unlike the Higgs propagator, Eq. (30), the correlator $\langle O(p)O(-p) \rangle$ is independent from the gauge parameter ξ .

4.2 Vectorial composite operators

We identify three gauge invariant vector composite operators, following the definitions of 't Hooft in [1], namely

$$\begin{aligned} O_\mu^3 &= i\phi^\dagger D_\mu \phi, \\ O_\mu^+ &= \phi^T \begin{pmatrix} 0 & 1 \\ -1 & 0 \end{pmatrix} D_\mu \phi, \\ O_\mu^- &= (O_\mu^+)^\dagger. \end{aligned} \tag{52}$$

The gauge invariance of O_μ^3 is apparent. For O_μ^+ , we can show the gauge invariance by using the following 2×2 matrix representation of a generic $SU(2)$ transformation,

$$U = \begin{pmatrix} a & -b^* \\ b & a^* \end{pmatrix} \tag{53}$$

with determinant $|a|^2 + |b|^2 = 1$. Thus, we find that under a $SU(2)$ transformation

$$\begin{aligned} O_\mu^+ &\rightarrow (U\phi)^T \begin{pmatrix} 0 & 1 \\ -1 & 0 \end{pmatrix} D_\mu(U\phi) \\ &= \phi^T U^T \begin{pmatrix} 0 & 1 \\ -1 & 0 \end{pmatrix} U D_\mu \phi \\ &= \phi^T \begin{pmatrix} 0 & 1 \\ -1 & 0 \end{pmatrix} D_\mu \phi = O_\mu^+, \end{aligned} \tag{54}$$

which shows the gauge invariance of O_μ^+ and, subsequently, of O_μ^- . After using the expansion (8), the first composite operator reads

$$\begin{aligned} O_\mu^3 &= i\phi^\dagger D_\mu \phi \\ &= i\phi^\dagger \partial_\mu \phi + \frac{1}{2} g \phi^\dagger \tau^a A_\mu^a \phi \\ &= \frac{i}{2} \left[(v+h)\partial_\mu h + i(v+h)\partial_\mu \rho^3 - i\rho^3 \partial_\mu h \right. \\ &\quad \left. + \rho^a \partial_\mu \rho^a + i\rho^1 \partial_\mu \rho^2 - i\rho^2 \partial_\mu \rho^1 \right. \\ &\quad \left. - \frac{i}{2} g(v+h)^2 A_\mu^3 + ig(v+h)(A_\mu^1 \rho^2 - A_\mu^2 \rho^1) \right. \\ &\quad \left. + \frac{i}{2} g\rho^a A_\mu^3 \rho^a - ig\rho^3 A_\mu^b \rho^b \right] \\ &= \frac{1}{2} \left[-(v+h)\partial_\mu \rho^3 + \rho^3 \partial_\mu h - \rho^1 \partial_\mu \rho^2 \right. \end{aligned}$$

$$\begin{aligned} &\left. + \rho^2 \partial_\mu \rho^1 + \frac{1}{2} g(v+h)^2 A_\mu^3 \right. \\ &\left. - g(v+h)(A_\mu^1 \rho^2 - A_\mu^2 \rho^1) \right. \\ &\left. - \frac{1}{2} g\rho^a A_\mu^3 \rho^a + g\rho^3 A_\mu^b \rho^b \right] + \frac{i}{2} \partial_\mu O, \end{aligned} \tag{55}$$

and since the last term, i.e. $\frac{i}{2} \partial_\mu O$, is BRST invariant, the sum of the others terms has to be BRST invariant too. Therefore, we can introduce the following three “reduced” vector composite operators R_μ^a with $a = 1, 2, 3$:

$$\begin{aligned} R_\mu^1 &= \frac{i}{2} (O_\mu^+ - O_\mu^-), \\ R_\mu^2 &= \frac{1}{2} (O_\mu^+ + O_\mu^-), \\ R_\mu^3 &= O_\mu^3 - \frac{i}{2} \partial_\mu O, \end{aligned} \tag{56}$$

so that

$$\begin{aligned} R_\mu^a &= \frac{1}{2} \left[-(v+h)\partial_\mu \rho^a + \rho^a \partial_\mu h - \varepsilon^{abc} \rho^b \partial_\mu \rho^c \right. \\ &\quad \left. + \frac{1}{2} g(v+h)^2 A_\mu^a - g(v+h)\varepsilon^{abc} (\rho^b A_\mu^c) \right. \\ &\quad \left. - \frac{1}{2} g A_\mu^a \rho^m \rho^m + g\rho^a A_\mu^m \rho^m \right], \end{aligned} \tag{57}$$

with R_μ^a both gauge and BRST invariant, thus

$$sR_\mu^a(x) = 0. \tag{58}$$

Notice that, as in the case of the scalar operator $O(x)$, the quantities $R_\mu^a(x)$ do not contain FP ghosts. Remarkably, the BRST invariant operators R_μ^a transform like a triplet under the custodial symmetry (20), namely

$$\delta R_\mu^a = \varepsilon^{abc} \rho^b R_\mu^c. \tag{59}$$

In work in progress [29], we shall see that the operators R_μ^a are the unique dimension three triplet vector operators belonging to the non-trivial BRST-cohomology and that they renormalize in the expected fashion [30], that is, up to BRST-exact terms and terms proportional to the equations of motion, complemented with contact terms to render their correlations fully finite, thereby generalizing the construct of [25].

Concerning the existence of possible mixings at the quantum level involving the vector composite operators R_μ^a , we can already anticipate here the output of the analysis which we shall present in detail in the forthcoming paper [29]. In particular, we have studied the cohomology of the BRST operator in the space of the local dimension three operators carrying a vector index as well as an $SU(2)$ index a , i.e. we have looked at the equation

$$s\Delta_\mu^a = 0 \tag{60}$$

with Δ_μ^a the most general local polynomial in the fields and their derivatives of dimension three, carrying a vector index as well as an $SU(2)$ index. After a quite lengthy analysis, it turns out that the most general solution of Eq. (60) is given by

$$\Delta_\mu^a = a_1 R_\mu^a + a_2 s(\epsilon^{abc} A_\mu^b \bar{c}^c) + a_3 s(i \partial_\mu \bar{c}^a). \tag{61}$$

where (a_1, a_2, a_3) are free coefficients. From the previous expression one sees that, unlike the $U(1)$ case in which the $U(1)$ vector operator V_μ can mix with $\partial_\nu F_{\mu\nu}$ (see [25]), in the non-Abelian case the operators R_μ^a can mix only with irrelevant BRST exact terms. The reasons behind this result are twofold. First, the non-Abelian analogue of $\partial_\nu F_{\mu\nu}$, i.e. $D_\nu^{ab} F_{\mu\nu}^b$, is not BRST invariant, rather it transforms covariantly, namely

$$s(D_\nu^{ab} F_{\mu\nu}^b) = \epsilon^{abc} D_\nu^{bd} F_{\mu\nu}^d c^c. \tag{62}$$

One sees thus that, unlike the operators R_μ^a , the quantity $D_\nu^{ab} F_{\mu\nu}^b$ does not enjoy the property of being strictly BRST invariant. As such, it cannot show up as a solution of Eq. (60).

The second reason is that, as it will be shown in details in the paper in preparation [29], the BRST vector operators R_μ^a are actually corresponding to the conserved Noether currents of the custodial symmetry, Eq. (20), an observation which has great consequences at the quantum level, being at the origin of a very powerful new local Ward identity which, much alike the $U(1)$ case (see [25]), enables us to work out the anomalous dimension of the operator R_μ^a in a purely algebraic way as well as to face the calculation of the correlator $\langle R_\mu^a(x) R_\mu^a(y) \rangle$ via Ward identities. As said before, all this will be presented in great details in the forthcoming paper [29].

Since the only rank two invariant tensor is δ^{ab} , we can write, moving to momentum space,

$$\begin{aligned} \langle R_\mu^a(p) R_\nu^b(-p) \rangle &= \delta^{ab} R_{\mu\nu}(p^2) \\ \rightarrow R_{\mu\nu}(p^2) &= \frac{1}{3} \langle R_\mu^a(p) R_\nu^a(-p) \rangle, \end{aligned} \tag{63}$$

as well as

$$R_{\mu\nu}(p^2) = R(p^2) \mathcal{P}_{\mu\nu}(p) + L(p^2) \mathcal{L}_{\mu\nu}(p), \tag{64}$$

so that in d dimensions,

$$R(p^2) = \frac{1}{3} \frac{\mathcal{P}_{\mu\nu}(p)}{(d-1)} \langle R_\mu^a(p) R_\nu^a(-p) \rangle, \tag{65}$$

and

$$L(p^2) = \frac{1}{3} \mathcal{L}_{\mu\nu}(p) \langle R_\mu^a(p) R_\nu^a(-p) \rangle. \tag{66}$$

One recognizes that Eqs. (63)–(66) display exactly the same structure of the gauge vector boson correlation function $\langle A_\mu^a(p) A_\nu^a(-p) \rangle$.

In the R_ξ -gauge, the non-vanishing contributions, up to first order in \hbar , to the correlation function $\langle R_\mu^a(p) R_\nu^b(-p) \rangle$ are

$$\begin{aligned} \langle R_\mu^a(p) R_\nu^a(-p) \rangle &= \frac{1}{16} g^2 v^4 \langle A_\mu^a(p) A_\nu^a(-p) \rangle \\ &\quad - \langle (\rho^a \partial_\mu h)(p) (\partial_\nu \rho^a h)(-p) \rangle \\ &\quad + \frac{1}{4} p_\mu p_\nu \langle (\rho^a h)(p) (\rho^a h)(-p) \rangle \\ &\quad + \frac{1}{8} p_\mu p_\nu \langle (\rho^a \rho^b)(p) (\rho^a \rho^b)(-p) \rangle \\ &\quad - \frac{1}{2} \langle (\rho^a \partial_\mu \rho^b)(p) (\partial_\nu \rho^a \rho^b)(-p) \rangle \\ &\quad + \frac{1}{4} g^2 v^3 \langle A_\mu^a(p) (A_\nu^a h)(-p) \rangle \\ &\quad - \frac{i}{4} g v^3 p_\nu \langle A_\mu^a(p) \rho^a(-p) \rangle \\ &\quad + \frac{1}{4} v^2 p_\mu p_\nu \langle \rho^a(p) \rho^a(-p) \rangle \\ &\quad + \frac{1}{6} g^2 v^2 \langle (\rho^a A_\mu^b)(p) (\rho^a A_\nu^b)(-p) \rangle \\ &\quad - \frac{1}{24} g^2 v^2 \langle (\rho^a \rho^a A_\mu^b)(p) A^b(-p) \rangle \\ &\quad + \frac{1}{8} g^2 v^2 \langle (h^2 A_\mu^a)(p) A_\nu^a(-p) \rangle \\ &\quad + \frac{1}{4} g^2 v^2 \langle (h A_\mu^a)(p) (h A_\nu^a)(-p) \rangle \\ &\quad + \frac{i}{4} v^2 g p_\mu \langle (h \rho^a)(p) A_\nu^a(-p) \rangle \\ &\quad + \frac{1}{2} g v^2 \langle (\partial_\mu h \rho^a)(p) A_\nu^a(-p) \rangle \\ &\quad + \frac{i}{2} g v^2 p_\mu \langle \rho^a(p) (h A_\nu^a)(-p) \rangle \\ &\quad - \frac{1}{4} g v^2 \epsilon^{abc} \langle A^a(p) (\rho^b \partial_\mu \rho^c)(-p) \rangle \\ &\quad - \frac{i g v^2}{2} \epsilon^{abc} p_\mu \langle \rho^a(p) (\rho^b A_\nu^c)(-p) \rangle \\ &\quad + \frac{1}{2} v p_\mu p_\nu \langle (h \rho^a)(p) \rho^a(-p) \rangle \\ &\quad - i v p_\nu \langle (\partial_\mu h \rho^a)(p) \rho^a(-p) \rangle. \end{aligned} \tag{67}$$

The first term in expression (67) is the gauge field propagator $\langle A_\mu^a(p) A_\nu^a(-p) \rangle$, which means that R_μ^a can be thought as a kind of BRST invariant extension of the elementary gauge field A_μ^a . At tree-level, we find in fact

$$\begin{aligned} \langle R_\mu^a(p) R_\nu^a(-p) \rangle_{tree} &= \frac{1}{16} g^2 v^4 \langle A_\mu^a(p) A_\nu^a(-p) \rangle \\ &\quad + \frac{1}{4} v^2 \partial_\mu \partial_\nu \langle \rho^a(p) \rho^a(-p) \rangle \\ &= \frac{3}{16} g^2 v^4 \frac{1}{p^2 + m^2} \mathcal{P}_{\mu\nu}(p) + \frac{3}{4} v^2 \mathcal{L}_{\mu\nu}(p), \end{aligned} \tag{68}$$

where we can see that, apart from the constant factor $\frac{3}{4}v^2$ appearing in the longitudinal sector, the transverse component reproduces exactly the transverse gauge tree-level propagator.

Collecting the results from Appendix E, we see that the transverse part of the correlator (65) in the R_ξ -gauge is

$$R(p^2) = \frac{1}{16}g^2v^4 \left(\frac{1}{p^2 + m^2} + \frac{1}{(p^2 + m^2)^2} \Pi_R(p^2) \right) + \mathcal{O}(\hbar^2) \tag{69}$$

where the divergent part of the one-loop correction is

$$\begin{aligned} \Pi_{R,\text{div}}(p^2) = & \frac{g^2}{\epsilon\pi^2} \left(-\frac{m_h^2 p^4}{32m^4} + \frac{9m^4}{16m_h^2} + \frac{9m^2 p^2}{8m_h^2} \right. \\ & \left. + \frac{m_h^2 p^2}{8m^2} + \frac{m_h^2}{16} - \frac{p^6}{48m^4} + \frac{23p^4}{96m^2} + \frac{7p^2}{8} \right), \end{aligned} \tag{70}$$

which is accounted for by appropriate counterterms in the $\overline{\text{MS}}$ -scheme renormalization procedure. Notice that, compatible with power counting, expression (70) is again a polynomial in p^2, v^2 upon re-instating the factored-out v^4 of Eq. (69).

We remain with

$$\begin{aligned} \Pi_R(p^2) = & \frac{3}{36\pi^2 g^2 v^4 m_h^2} \int_0^1 dx \left\{ 6m^4 (m_h^4 + 3m^4) \right. \\ & - \frac{p^4 m_h^2}{3} (9m_h^2 + 35m^2 + 4p^2) \\ & + p^2 (m^4 m_h^2 + 10m^2 m_h^4 + m_h^6 + 36m^6) \\ & + m_h^4 (-p^2 (m_h^2 + 11m^2) - 6m^4 + p^4) \ln \left(\frac{m_h^2}{\mu^2} \right) \\ & + m_h^2 (2p^4 (m_h^2 - 5m^2) + (m^2 - m_h^2)^2 p^2 + p^6) \\ & \times \ln \left(\frac{p^2(1-x)x + (1-x)m_h^2 + xm^2}{\mu^2} \right) \\ & + m_h^2 (48m^6 - 68m^4 p^2 - 16m^2 p^4 + p^6) \\ & \times \ln \left(\frac{p^2(1-x)x + m^2}{\mu^2} \right) \\ & + m^2 (m_h^2 (-48m^4 - 17m^2 p^2 + 3p^4) \\ & \left. + p^2 m_h^4 - 54 (m^6 + 2m^4 p^2)) \ln \left(\frac{m^2}{\mu^2} \right) \right\}. \end{aligned} \tag{71}$$

Since (71) contains terms of the order of $\frac{p^4}{(p^2+m^2)^2} \ln(p^2)$ and $\frac{p^6}{(p^2+m^2)^2} \ln(p^2)$, we follow the steps (36)–(38) to find the resummed propagator in the one-loop approximation,

namely

$$G_R(p^2) = \frac{1}{16}g^2v^4 \left(\frac{1}{p^2 + m_h^2 - \hat{\Pi}_R(p^2)} \right) + C_R(p^2) \tag{72}$$

with

$$\begin{aligned} \hat{\Pi}_R(p^2) = & \frac{3}{36\pi^2 g^2 v^4 m_h^2} \int_0^1 dx \left\{ 6m^4 (m_h^4 + 3m^4) \right. \\ & - \frac{p^4 m_h^2}{3} (9m_h^2 + 35m^2 + 4p^2) \\ & + p^2 (m^4 m_h^2 + 10m^2 m_h^4 + m_h^6 + 36m^6) \\ & + m_h^4 (-p^2 (m_h^2 + 11m^2) \\ & - 6m^4 + p^4) \ln \left(\frac{m_h^2}{\mu^2} \right) \\ & + m_h^2 (m_h^4 p^2 - 2m_h^2 m^4 - 6m_h^2 m^2 p^2 + 12m^6 + 24m^4 p^2) \\ & \times \ln \left(\frac{x(m^2 - p^2(x-1)) - (x-1)m_h^2}{\mu^2} \right) \\ & + 33m_h^2 (2m^6 - m^4 p^2) \ln \left(\frac{m^2 - p^2(x-1)x}{\mu^2} \right) \\ & + m^2 (m_h^2 (-48m^4 - 17m^2 p^2 + 3p^4) + p^2 m_h^4 \\ & \left. - 54 (m^6 + 2m^4 p^2)) \ln \left(\frac{m^2}{\mu^2} \right) \right\} \end{aligned} \tag{73}$$

and

$$\begin{aligned} C_R(p^2) = & \frac{1}{12(4\pi)^2} \int_0^1 dx \left\{ (-18m^2 + p^2) \right. \\ & \times \ln \left(\frac{p^2(1-x)x + m^2}{\mu^2} \right) + ((2m_h^2 - 6m^2) + p^2) \\ & \left. \times \ln \left(\frac{p^2 x(1-x) + (1-x)m_h^2 + xm^2}{\mu^2} \right) \right\}. \end{aligned} \tag{74}$$

Looking now at the longitudinal part $L(p^2)$, it turns out to be

$$\begin{aligned} L(p^2) = & \frac{1}{4}v^2 \\ & - \frac{1}{(4\pi)^2} \left(\frac{m_h^4 - 3m_h^4 \ln \left(\frac{m_h^2}{\mu^2} \right) + 9m^4 - 27m^4 \ln \left(\frac{m^2}{\mu^2} \right)}{2m_h^2} \right. \\ & \left. - \frac{1}{\epsilon} \left(m_h^2 - 9 \frac{m^4}{m_h^2} \right) \right). \end{aligned} \tag{75}$$

As it happens in the tree-level case, expression (75) is independent from the momentum p^2 , meaning that it does not correspond to the propagation of some physical mode, a feature which is expected to be valid in general. This will be discussed elsewhere, as it requires an in-depth analysis of

non-trivial Ward identities and their consequent restrictions on the correlation functions of the composite operators.

5 Spectral properties

In this section, we will calculate the spectral properties associated with the correlation functions obtained in the last section. In Sect. 5.1, we will shortly remind the techniques employed in [23] to obtain the pole mass, residue and spectral density up to first order in \hbar . In Sect. 5.2.2, we analyze the spectral properties of the elementary fields. In Sect. 5.4, the spectral properties of the composite operators $O(x)$ and $R_\mu^a(x)$ are discussed.

5.1 Obtaining the spectral function

We compare the Källén-Lehmann³ spectral representation for the propagator of a generic field $\tilde{O}(p)$

$$\langle \tilde{O}(p)\tilde{O}(-p) \rangle = G(p^2) = \int_0^\infty dt \frac{\rho(t)}{t + p^2}, \tag{76}$$

where $\rho(t)$ is the spectral density function and $G(p^2)$ stands for the resummed propagator

$$G(p^2) = \frac{1}{p^2 + m^2 - \Pi(p^2)}. \tag{77}$$

The pole mass for any massless or massive field excitation is obtained by calculating the pole of the resummed propagator, that is, by solving

$$p^2 + m^2 - \Pi(p^2) = 0 \tag{78}$$

and its solution defines the pole mass $p^2 = -m_{\text{pole}}^2$. As consistency requires us to work up to a fixed order in perturbation theory, we should solve Eq. (78) for the pole mass in an iterative fashion. Therefore, to first order in \hbar , we find

$$m_{\text{pole}}^2 = m^2 - \Pi^{1\text{-loop}}(-m^2) + \mathcal{O}(\hbar^2), \tag{79}$$

³ We remind here that in the case of higher dimensional operators, the spectral representation, Eq. (76), might require appropriate subtraction terms in order to ensure convergence. A standard way to cure this problem is to subtract from $G(p^2)$ the first few terms of its Taylor expansion at $p = 0$ [31], leading to $G^{(n)}(p^2) = (-p^2)^n \int dt \frac{\rho(t)}{(t^n(t+p^2))}$ in the n th subtraction, making the integral more and more convergent. In our theory we can make use of the subtracted equations at $p^2 = 0$ because all fields are massive in the R_ξ -gauge, so there are no divergences at zero momentum. These polynomial subtraction terms are in a direct correspondence with the aforementioned contact terms necessary to render the composite operator's correlation functions finite, see [25] for more on this.

where $\Pi^{1\text{-loop}}$ is the first order, or one-loop, correction to the propagator. Now, we write Eq. (77) in a slightly different way, namely

$$\begin{aligned} G(p^2) &= \frac{1}{p^2 + m^2 - \Pi(p^2)} \\ &= \frac{1}{p^2 + m^2 - \Pi^{1\text{-loop}}(-m^2) - (\Pi(p^2) - \Pi^{1\text{-loop}}(-m^2))} \\ &= \frac{1}{p^2 + m_{\text{pole}}^2 - \tilde{\Pi}(p^2)}, \end{aligned} \tag{80}$$

where we defined $\tilde{\Pi}(p^2) = \Pi(p^2) - \Pi^{1\text{-loop}}(-m^2)$. At one-loop, expanding $\tilde{\Pi}(p^2)$ around $p^2 = -m_{\text{pole}}^2 = -m^2 + \mathcal{O}(\hbar)$ gives the residue

$$\begin{aligned} Z &= \lim_{p^2 \rightarrow -m_{\text{pole}}^2} (p^2 + m_{\text{pole}}^2)G(p^2) \\ &= \frac{1}{1 - \partial_{p^2}\Pi(p^2)|_{p^2=-m^2}} \\ &= 1 + \partial_{p^2}\Pi(p^2)|_{p^2=-m^2} + \mathcal{O}(\hbar^2). \end{aligned} \tag{81}$$

We now write (80) to first order in \hbar as

$$\begin{aligned} G(p^2) &= \frac{Z}{(p^2 + m_{\text{pole}}^2 - \tilde{\Pi}(p^2))Z} \\ &= \frac{Z}{p^2 + m_{\text{pole}}^2 - \tilde{\Pi}(p^2) + (p^2 + m_{\text{pole}}^2) \frac{\partial \tilde{\Pi}(p^2)}{\partial p^2} |_{p^2=-m^2}} \\ &= \frac{Z}{p^2 + m_{\text{pole}}^2} \\ &\quad + Z \left(\frac{\tilde{\Pi}(p^2) - (p^2 + m_{\text{pole}}^2) \frac{\partial \tilde{\Pi}(p^2)}{\partial p^2} |_{p^2=-m^2}}{(p^2 + m_{\text{pole}}^2)^2} \right), \end{aligned} \tag{82}$$

where in the last line we used a first-order Taylor expansion so that the propagator has an isolated pole at $p^2 = -m_{\text{pole}}^2$. In (76) we can isolate this pole in the same way, by defining the spectral density function as $\rho(t) = Z\delta(t - m_{\text{pole}}^2) + \tilde{\rho}(t)$, giving

$$G(p^2) = \frac{Z}{p^2 + m_{\text{pole}}^2} + \int_0^\infty dt \frac{\tilde{\rho}(t)}{t + p^2} \tag{83}$$

and we identify the second term in each of the representations (82) and (83) as the *reduced propagator*

$$\tilde{G}(p^2) \equiv G(p^2) - \frac{Z}{p^2 + m_{\text{pole}}^2}, \tag{84}$$

so that

$$\begin{aligned} \tilde{G}(p^2) &= \int_0^\infty dt \frac{\tilde{\rho}(t)}{t + p^2} \\ &= Z \left(\frac{\tilde{\Pi}(p^2) - (p^2 + m_{\text{pole}}^2) \frac{\partial \tilde{\Pi}(p^2)}{\partial p^2} |_{p^2=-m^2}}{(p^2 + m_{\text{pole}}^2)^2} \right). \end{aligned} \tag{85}$$

Finally, using Cauchy’s integral theorem from complex analysis, we can find the spectral density $\tilde{\rho}(t)$ as a function of $\tilde{G}(p^2)$, giving

$$\tilde{\rho}(t) = \frac{1}{2\pi i} \lim_{\epsilon \rightarrow 0^+} (\tilde{G}(-t - i\epsilon) - \tilde{G}(-t + i\epsilon)). \tag{86}$$

5.1.1 Pole masses

There is an interesting consequence of the definition of the first-order pole mass, Eq. (79). When calculating one-loop corrections to the two-point function of the composite operators $O(p)$ and $R_\mu^a(p)$, we find that

$$\begin{aligned} \Pi_{\text{composite}}(p^2) &= \Pi_{\text{elementary}}(p^2) + \Pi_{1\text{-leg}}(p^2)(p^2 + m^2) \\ &\quad + \Pi_{0\text{-leg}}(p^2)(p^2 + m^2)^2, \end{aligned} \tag{87}$$

where $\Pi_{1\text{-leg}}(p^2)$ and $\Pi_{0\text{-leg}}(p^2)$ are the composite one-loop contributions to the correction of the composite field’s two-point functions, with one external leg and zero external legs, respectively. From this, we see immediately that

$$\Pi_{\text{composite}}(-m^2) = \Pi_{\text{elementary}}(-m^2) \tag{88}$$

and therefore, up to first order in \hbar , we find

$$m_{\text{pole, composite}}^2 = m_{\text{pole, elementary}}^2 \tag{89}$$

which means that the elementary operators and their composite extensions share the same mass. We remind here that the order-per-order gauge parameter independence of the pole masses in the elementary correlation functions $\langle A_\mu^a(x) A_\nu^b(y) \rangle$ and $\langle h(x) h(y) \rangle$ can also be shown using the Nielsen identities, which themselves can be derived from the Slavnov–Taylor identity following the BRST tools of e.g. [9, 11], see also [23] for an explicit verification in the $U(1)$ case. This is an important feature, providing an alternative way to the Nielsen identities, to understand why the pole masses of the elementary particles are gauge invariant and not just gauge parameter independent.

5.2 Spectral properties of the elementary fields

We first discuss the spectral properties of the elementary fields: the scalar Higgs field $h(x)$ and the transverse part of the gauge field $A_\mu^a(x)$. We will work with two sets of parameters, set out in Table 1. All values are given in units of the energy scale μ . Also, we have that $m^2 = \frac{1}{4}g^2v^2$ and

Table 1 Parameter values used in the spectral density functions

	Region I	Region II
v	0.8μ	1μ
g	1.2	0.5
λ	0.3	0.205

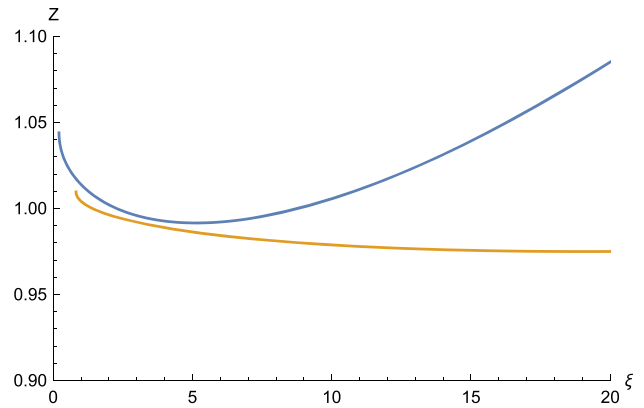


Fig. 1 Dependence of the residue Z for the Higgs field propagator on the gauge parameter ξ , for Region I (blue), and Region II (orange)

$m_h^2 = \lambda v^2$, so that $m^2 = 0.23 \mu^2$ and $m_h^2 = 0.192 \mu^2$ in Region I and $m^2 = 0.625 \mu^2$ and $m_h^2 = 0.205 \mu^2$ in Region II.

5.2.1 The Higgs field

For the Higgs fields, following the steps from Sect. 5.1, we find the pole mass to first order in \hbar to be: for Region I

$$m_{\hbar, \text{pole}}^2 = 0.207 \mu^2, \tag{90}$$

and for Region II

$$m_{\hbar, \text{pole}}^2 = 0.206 \mu^2, \tag{91}$$

for all values of the parameter ξ . This means that while the Higgs propagator (24) is gauge dependent, the pole mass is gauge independent. This is in full agreement with the Nielsen identities of the $SU(2)$ Higgs model studied in [10]. The residue, however, is gauge dependent, as is depicted in Fig. 1. For small values of ξ , including the Landau gauge $\xi = 0$, the residue is not well-defined, and we cannot determine the spectral density function, as we will explain further in the next section.

In Fig. 2, we find the spectral density functions both regions, for three values of $\xi : 1, 2, 5$. Looking at Region I, we see the first two-particle state appearing at $t = (m_h + m_h)^2 = 0.768 \mu^2$, followed by another two-particle state at $t = (m + m)^2 = 0.922 \mu^2$. Then, we see that there is a negative contribution, different for each diagram, at $t = (\sqrt{\xi}m + \sqrt{\xi}m)^2$. This corresponds to the (unphysical) two-particle state of two Goldstone bosons. For $\xi < 3$, this leads to a negative contribution for the spectral function, probably due to the large-momentum behaviour of the Higgs propagator (24), for a detailed discussion see [23]. For Region II, we find essentially the same behaviour: a Higgs two-particle state at $t = (m_h + m_h)^2 = 0.81 \mu^2$, and a gauge field two-particle state at $t = (m + m)^2 = 0.25 \mu^2$. We

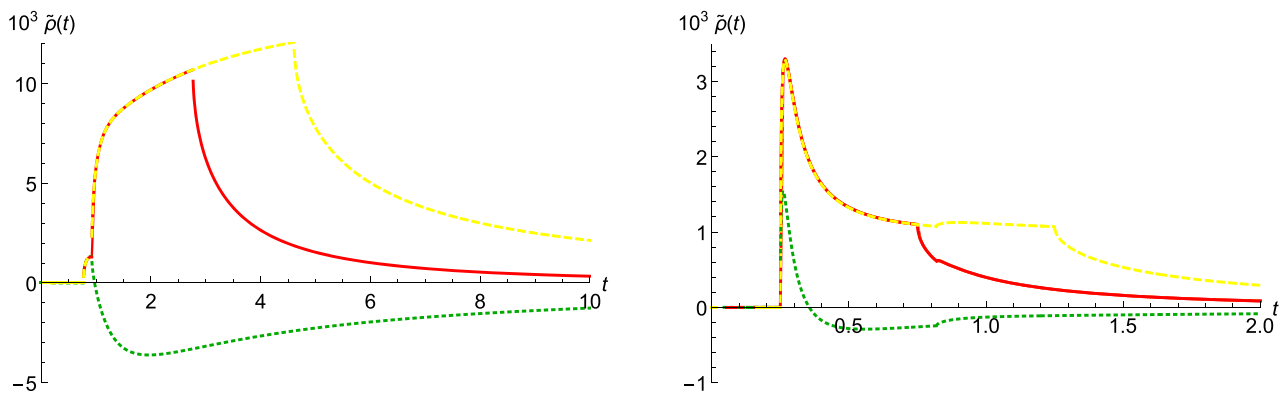


Fig. 2 Spectral functions for the propagator $\langle h(p)h(-p) \rangle$, for $\xi = 1$ (green, dotted), $\xi = 3$ (red, solid), $\xi = 5$ (yellow, dashed), with t given in units of μ^2 , for Region I (left) and Region II (right) with the parameter values given in Table 1

also see a negative contribution different for each diagram at $t = (\sqrt{\xi}m + \sqrt{\xi}m)^2$, corresponding to the (unphysical) two-particle state of two Goldstone bosons.

5.2.2 The transverse gauge field

For the gauge field propagator, following the steps from Sect. 5.1, we find the first-order pole mass of the transverse gauge field to be: for Region I

$$m_{\text{pole}}^2 = 0.274 \mu^2 \tag{92}$$

and for Region II

$$m_{\text{pole}}^2 = 0.065 \mu^2 \tag{93}$$

for all values of the parameter ξ , so that the pole mass is independent from the gauge parameter. The residue is, however, gauge dependent as is depicted in Fig. 3. For small values of ξ the residue is not well-defined, as we will explain further in the next section.

In Fig. 4, we find the spectral density functions for both regions, for three values of ξ : 1, 2, 5. Looking at Region I, we see the first two-particle state appearing at $t = (m_h + m)^2 = 0.843 \mu^2$, followed by a two-particle state at $t = (m + m)^2 = 0.922 \mu^2$. Then, we see that there is a negative contribution, different for each diagram, at $t = (m + \sqrt{\xi}m)^2$. This corresponds to the (unphysical) two-particle state of a gauge and Goldstone boson. For Region II, we find a gauge field two-particle state at $t = (m + m)^2 = 0.25 \mu^2$. We also see a negative contribution different for each diagram at $t = (m + \sqrt{\xi}m)^2$, corresponding to the (unphysical) two-particle state of two Goldstone bosons.

5.3 Unphysical threshold effects

From the Feynman vertex rules given in Appendix A, for certain values of the masses, unphysical threshold effects

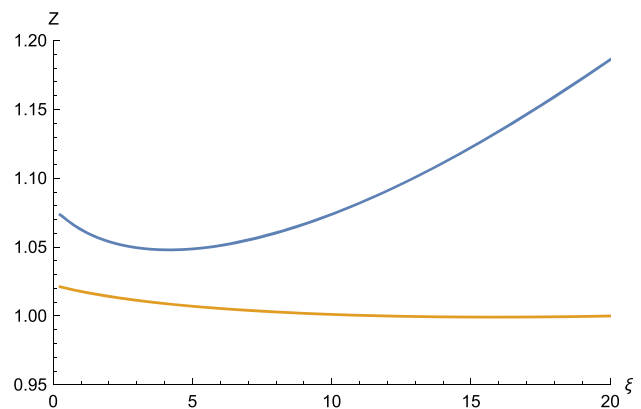


Fig. 3 Dependence of the residue Z for the gauge field propagator from the gauge parameter ξ , for Region I (blue), and Region II (orange)

can occur. These effects imply that for certain values of the (physical and unphysical) parameters, a “decay” occurs of a gauge and Higgs boson into two other particles, see Fig. 5. We distinguish three cases:

1. Decay of a gauge vector boson in two Goldstone bosons: this happens when $m > 2\sqrt{\xi}m$.
2. Decay of a Higgs boson in two gauge vector bosons: this happens when $m_h > 2m$.
3. Decay of a Higgs boson in two Goldstone bosons: this happens when $m_h > 2\sqrt{\xi}m$.

In order to guarantee the stability of the gauge boson, we therefore need from (1) that $\xi > \frac{1}{4}$. This means that for the Landau gauge $\xi = 0$, the elementary gauge boson is not stable. For the Higgs particle, to guarantee stability we need from (2) that $m_h < 2m$. Then, from (3) we find that $\xi > \frac{m_h^2}{4m^2}$. This is the window in which we can work with a

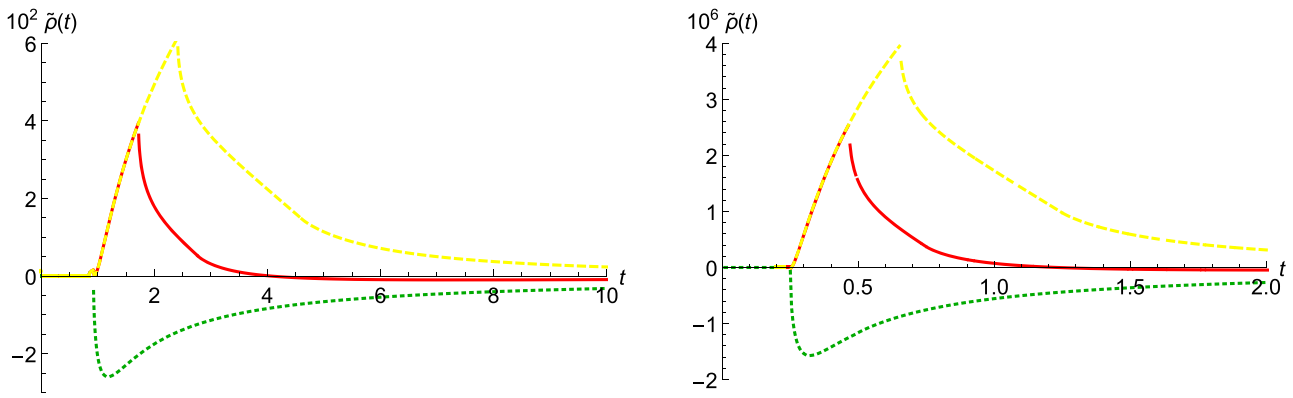


Fig. 4 Spectral functions for the propagator $\langle A_\mu^a(p)A_\nu^b(-p) \rangle^T$, for $\xi = 1$ (green, dotted), $\xi = 3$ (red, solid), $\xi = 5$ (yellow, dashed), with t given in units of μ^2 , for Region I (left) and Region II (right) with the parameter values given in Table 1

stable model. We can have a look at what happens when we go outside of this window. For the Higgs particle, we see that for $m_h > 2m$, or $\lambda < g^2$, we will find a complex value for the first order pole mass, calculated through (78). For $\lambda \geq g^2$, we will always find a real pole mass. Since the pole mass is gauge invariant, we find that this is true for all values of ξ . However, we do find that for $\xi > \frac{m_h^2}{4m^2}$ and $\lambda > g^2$, the real value of the pole mass is a real point inside the branch cut. This means that we cannot achieve the usual differentiation around this point. As a consequence, we cannot consistently construct the residue, so that we are unable to obtain a first-order spectral function. For the gauge field, we find the same problem when $\xi < \frac{1}{4}$.

The foregoing mathematically correct observations clearly show that there is something physically wrong with using the elementary fields' spectral functions. Luckily, all of these shortcomings are surpassed by using the gauge invariant composite operators.

5.4 Spectral properties for the composite fields

For the scalar composite operator $O(x)$, whose two-point function is given by expression (48), we find the first-order pole mass for Region I

$$m_{O,\text{pole}}^2 = 0.207 \mu^2, \tag{94}$$

and for Region II

$$m_{O,\text{pole}}^2 = 0.206 \mu^2, \tag{95}$$

which is equal to the pole mass of the elementary Higgs field in (90), as we expect from Eq. (89). Following the steps from Sect. 5.1, we find the first-order residue

$$Z = 1.11 v^2 \tag{96}$$

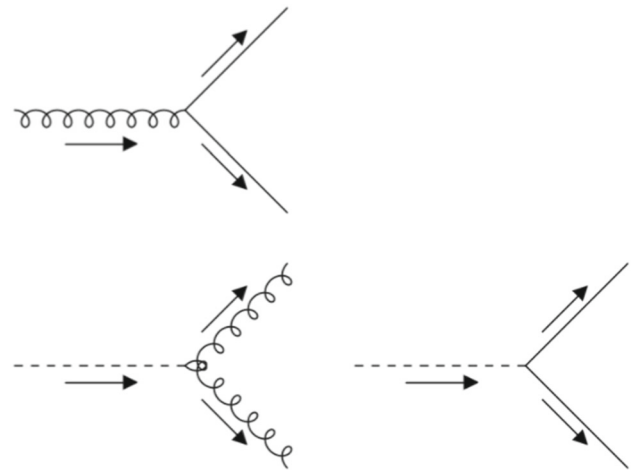


Fig. 5 Possible decays of the gauge boson (above) and the Higgs boson (below). The arrows indicate the momentum flow

for Region I and

$$Z = 1.01 v^2 \tag{97}$$

for Region II. The first order spectral function for $\langle O(x) O(y) \rangle$ is shown in Fig. 6. Comparing this result with that of the spectral function of the Higgs field in Fig. 4, we see a two-particle state for the Higgs field at $t = (m_h + m_h)^2$, and a two-particle state for the gauge vector field, starting at $t = (m + m)^2$. The difference is that for the gauge invariant correlation function $\langle O(x) O(y) \rangle$ we no longer have the unphysical Goldstone two-particle state. Due to the absence of this negative contribution, the spectral function is positive throughout the spectrum. In fact, we see that for bigger values of ξ , we find that the spectral function of the elementary Higgs field resembles more and more the spectral function of the composite operator $O(x)$. This makes sense, since for $\xi \rightarrow \infty$, we are approaching the unitary gauge which has a more direct link

with the physical spectrum of the elementary excitations. In Appendix G, one finds a detailed discussion about the unitary gauge limit $\xi \rightarrow \infty$ as well as the calculation of the spectral function. Of course, the unitary gauge is not well-suited for computations at the quantum level due to the non-renormalizability issue in general, and non-curable overlapping divergences in particular, but for gauge invariant quantities, it was already noted in [32] that (for the β -functions) the unitary gauge choice can still be useful, at least up to one-loop order. Therefore, in Appendix G, we have analyzed, at one-loop order where there are no overlapping divergences yet, the scalar and vector correlation functions directly in the unitary gauge and we do find that their *finite* pieces are identical to those obtained in the R_ξ -gauge discussed so far. Given that several propagators are trivial in the unitary gauge, the computations in the latter gauge are evidently far more economical. A similar observation was already made in the $U(1)$ case as well, see [25].

The asymptotic (constant) behaviour is directly related to the (classical) dimension of the used composite operator.

5.4.1 The vector composite operator $R_\mu^a(x)$

For the transverse part of the two-point correlation function $G_R(p^2)$, Eq. (72), for our set of parameters we find the first-order pole mass: in Region I

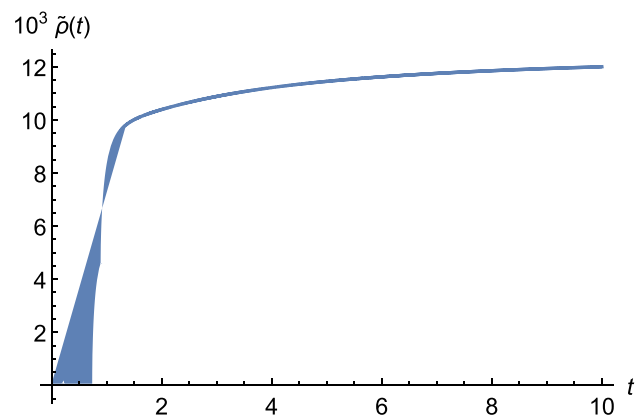
$$m_{R,\text{pole}}^2 = 0.274 \mu^2 \tag{98}$$

and Region II

$$m_{R,\text{pole}}^2 = 0.065 \mu^2 \tag{99}$$

which is the same as the pole mass of the transverse gauge field, Eq. (92), in agreement with Eq. (89). Following the steps from 5.1, we find the first-order residue

$$Z = \frac{1}{16} g^2 v^4 \tag{100}$$



for Region I and

$$Z = \frac{1}{16} g^2 v^4 \tag{101}$$

for Region II. The first order spectral function for $G_R(p^2)$ is shown in Fig. 7. Comparing this to the spectral function of the gauge vector field in Fig. 4, we see a two-particle state at $t = (m_h + m)^2$, and a two-particle state for the gauge field, starting at $t = (m+m)^2$. Again, as in the case of the two-point correlation function of the scalar operator $O(x)$, the difference is that for this gauge invariant correlation function we no longer have the unphysical Goldstone/gauge boson two-particle state. Due to the absence of this negative contribution, the spectral function is positive throughout the spectrum. In fact, we see that for bigger values of ξ , we find that the spectral function of the elementary gauge field resembles more and more the spectral function of the composite operator $R_\mu^a(x)$. As already mentioned previously, this relies on the fact that in the limit $\xi \rightarrow \infty$ we are approaching the unitary gauge, see Appendix G. Also here, the linear increase at large t follows from the operator dimension.

6 Conclusion and outlook

This work is the natural extension of previous studies [23–25], where the Abelian $U(1)$ Higgs model has been scrutinized by employing two local composite BRST invariant operators [1, 14, 15], whose two-point correlation functions provide a fully gauge independent description of the elementary excitations of the model, namely the Higgs and the massive gauge boson.

This formulation generalizes to the non-Abelian Higgs model as, for example, the $SU(2)$ Yang–Mills theory with a single Higgs in the fundamental representation [1, 14, 15]. This is the model which has been considered in the present analysis. The local gauge and BRST invariant composite

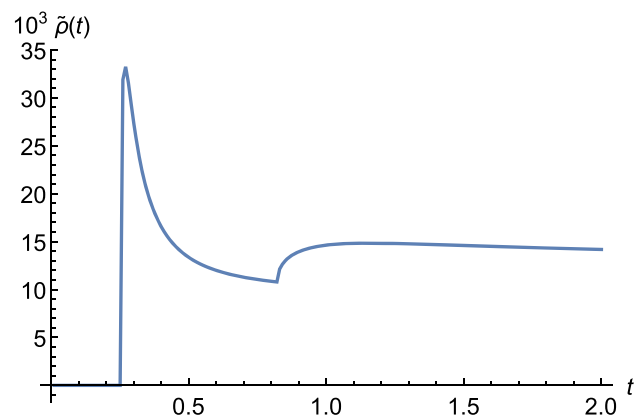


Fig. 6 Spectral function for the two-point correlation function $\langle O(p)O(-p) \rangle$, with t given in units of μ^2 , for the Region I (left) and Region II (right) with parameter values given in Table 1

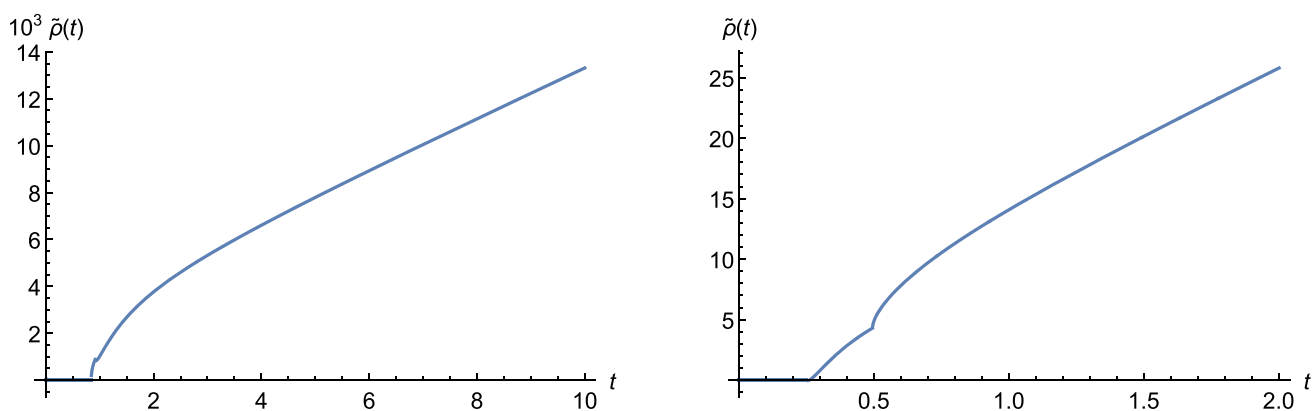


Fig. 7 Spectral function for the transverse two-point correlation function $G_R(p^2)$, with t given in units of μ^2 , for the Region I (left) and Region II (right) with parameter values given in Table 1

operators ($O(x)$, $R_\mu^a(x)$) which generalize their $U(1)$ counterparts are given in Eq. (43) and in Eqs. (56) and (57).

The two-point correlation functions $\langle O(x)O(y) \rangle$ and $\langle R_\mu^a(x)R_\nu^b(y) \rangle^T$, where the superscript T stands for the transverse component, have been evaluated at one-loop order in the R_ξ -gauge and compared with the corresponding correlation functions of the elementary fields $\langle h(x)h(y) \rangle$ and $\langle A_\mu^a(x)A_\nu^b(y) \rangle^T$. It turns out that both $\langle O(x)O(y) \rangle$ and $\langle h(x)h(y) \rangle$ share the same gauge independent pole mass, Eqs. (90), (91), (94) and (95), in agreement with both Nielsen identities [7–13] and the BRST invariant nature of $O(x)$. Nevertheless, unlike the residue and spectral function of the elementary correlator $\langle h(x)h(y) \rangle$, which exhibit a strong unphysical dependence from the gauge parameter ξ , Fig. 2, the spectral density of $\langle O(x)O(y) \rangle$ turns out to be ξ -independent and positive over the whole p^2 axis, Fig. 6. The same features hold for $\langle A_\mu^a(x)A_\nu^b(y) \rangle^T$ and $\langle R_\mu^a(x)R_\nu^b(y) \rangle^T$. Again, both correlation function share the same ξ -independent pole mass, Eqs. (92), (93), (98) and (99). Though, unlike the ξ -dependent spectral function associated to $\langle A_\mu^a(x)A_\nu^b(y) \rangle^T$, Fig. 4, that corresponding to $\langle R_\mu^a(x)R_\nu^b(y) \rangle^T$, Fig. 7, turns out to be independent from the gauge parameter ξ and positive. As such, the local composite operators ($O(x)$, $R_\mu^a(x)$) provide a fully BRST consistent description of the observable scalar (Higgs) and vector boson particles.

It is worth mentioning here that, besides the BRST invariance of the gauge fixed action, the model exhibits an additional global custodial symmetry, Eqs. (20) and (21), according to which all fields carrying the index $a = 1, 2, 3$, i.e. $(A_\mu^a, b^a, c^a, \bar{c}^a, \rho^a)$, undergo a global transformation in the adjoint representation of $SU(2)$. The same feature holds for the composite operators ($O(x)$, $R_\mu^a(x)$) which transform exactly as h and A_μ^a . More precisely, the operator $O(x)$ is a singlet under the custodial symmetry, while the operators R_μ^a transform like a triplet, Eq. (59), so that the correlation

function $\langle R_\mu^a(p)R_\nu^b(-p) \rangle$ displays the same $SU(2)$ structure of the elementary two-point function $\langle A_\mu^a(p)A_\nu(-p) \rangle$, Eqs. (63)–(66). Although not being the aim of the present analysis, we expect that the existence of a global custodial symmetry will imply far-reaching consequences for the renormalization properties of the composite operators ($O(x)$, $R_\mu^a(x)$) encoded in the corresponding Ward identities, allowing a generalization of the $U(1)$ renormalizability analysis of [25].

The analysis of the spectral properties of the operators ($O(x)$, $R_\mu^a(x)$) worked out here could pave the route for more ambitious projects which might lead to an interesting interplay with possible future investigation on the lattice of the correlators $\langle O(x)O(y) \rangle$ and $\langle R_\mu^a(x)R_\nu^b(y) \rangle^T$, as already mentioned in [16, 17]. The BRST invariant nature of ($O(x)$, $R_\mu^a(x)$) makes them natural candidates to attempting at facing the challenge of investigating the infrared non-perturbative behaviour of the model, trying to make contact with the analytical lattice predictions of Fradkin and Shenker [33], see also [34] for a general overview and [35] for a new take on these matters. This study would enable us to shed some light on the issue of the positivity of the spectral densities in the non-perturbative region, a topic which is currently under intensive investigation in confining Yang–Mills theories without the presence of Higgs fields, see [36–73]. Finally, it would be worth to investigate to which extent the BRST invariant correlation functions $\langle O(x)O(y) \rangle$, $\langle R_\mu^a(x)R_\nu^b(y) \rangle^T$ could be affected by the existence of the non-perturbative effect of the Gribov copies, by means of the recent BRST invariant formulation of the (Refined) Gribov–Zwanziger horizon function [74, 75].

Another most promising avenue to further explore is the $SU(2) \times U(1)$ setting of the electroweak theory, where the gauge invariant description of electric charge will necessitate the combination of the (local) gauge invariant composite operators set out here and (non-local) dressed gauge invariant operators, see [76].

Acknowledgements The authors would like to thank the Brazilian agencies CNPq and FAPERJ for financial support. This study was financed in part by the Coordenação de Aperfeiçoamento de Pessoal de Nível Superior - Brasil (CAPES) - Finance Code 001. This paper is also part of the project INCT-FNA Process No. 464898/2014-5. S.P. Sorella is a level 1 CNPq researcher under the contract 301030/2019-7. M.S. Guimaraes is a level 2 CNPq researcher under the contract 307801/2017-9 and L.F. Palhares is a level 2 CNPq researcher under the contract 311751/2019-9.

Data Availability Statement This manuscript has no associated data or the data will not be deposited. [Authors' comment: Our plots are all direct output from our analytical computations, as such we do not have any associated data to deposit.]

Open Access This article is licensed under a Creative Commons Attribution 4.0 International License, which permits use, sharing, adaptation, distribution and reproduction in any medium or format, as long as you give appropriate credit to the original author(s) and the source, provide a link to the Creative Commons licence, and indicate if changes were made. The images or other third party material in this article are included in the article's Creative Commons licence, unless indicated otherwise in a credit line to the material. If material is not included in the article's Creative Commons licence and your intended use is not permitted by statutory regulation or exceeds the permitted use, you will need to obtain permission directly from the copyright holder. To view a copy of this licence, visit <http://creativecommons.org/licenses/by/4.0/>.
Funded by SCOAP³.

Appendix A: Propagators and vertices

The tree level elementary propagators of the fields are easily computed, for example by coupling a source J_φ to each field φ and computing at leading order the functional derivative $\frac{\delta^2 Z^c}{\delta J_\varphi(-p)\delta J_\varphi(p)}$ with Z^c the generating functional of connected two-point functions. This leads to

$$\begin{aligned} \langle A_\mu^a(p)A_\nu^b(-p) \rangle &= \frac{\delta^{ab}}{p^2 + m^2} \mathcal{P}_{\mu\nu}(p) \\ &\quad + \delta^{ab} \frac{\xi}{p^2 + \xi m^2} \mathcal{L}_{\mu\nu}(p), \\ \langle \rho^a(p)\rho^b(-p) \rangle &= \frac{\delta^{ab}}{p^2 + \xi m^2}, \\ \langle h(p)h(-p) \rangle &= \frac{1}{p^2 + m_h^2}, \\ \langle A_\mu^a(p)b^b(-p) \rangle &= \delta^{ab} \frac{p_\mu}{p^2 + \xi m^2}, \\ \langle b^a(p)\rho^b(-k) \rangle &= \delta^{ab} \frac{im}{p^2 + \xi m^2} \end{aligned} \tag{A1}$$

and

$$\langle \bar{c}^a(p)c^b(-p) \rangle = \frac{\delta^{ab}}{p^2 + \xi m^2} \tag{A2}$$

for the ghost propagator. All other propagators are zero. This includes the mixed propagator, $\langle A_\mu^a(x)\rho^b(y) \rangle = 0$, a well-known feature of the R_ξ -gauge [2, Chap. 21].

For all vertices, adopting the convention that the momentum is flowing towards the vertex, we get

- The AAh -vertex: $\Gamma_{A_\mu^a A_\nu^b h}(-p_1, -p_2, -p_3) = -\frac{g^2 v}{2} \delta_{\mu\nu} \delta^{ab} \delta(p_1 + p_2 + p_3)$.
- The $\rho\rho A$ -vertex: $\Gamma_{\rho^a \rho^b A_\mu^c}(-p_1, -p_2, -p_3) = \frac{g}{2} i \epsilon^{abc} (p_{\mu,1} - p_{\mu,2}) \delta(p_1 + p_2 + p_3)$.
- The $A\rho h$ -vertex: $\Gamma_{A_\mu^a \rho^b h}(-p_1, -p_2, -p_3) = i \frac{g}{2} \delta^{ab} (p_{\mu,3} - p_{\mu,2}) \delta(p_1 + p_2 + p_3)$.
- The hhh vertex: $\Gamma_{hhh}(-p_1, -p_2, -p_3) = -3\lambda v \delta(p_1 + p_2 + p_3)$.
- The $h\rho\rho$ vertex: $\Gamma_{h\rho^a \rho^b}(-p_1, -p_2, -p_3) = -\lambda v \delta^{ab} \delta(p_1 + p_2 + p_3)$.
- The AAA -vertex: $\Gamma_{A_\mu^a A_\nu^b A_\sigma^c}(-p_1, -p_2, -p_3) = -i g f^{abc} [(p_1 - p_3)_\nu \delta_{\sigma\mu} + (p_3 - p_2)_\mu \delta_{\nu\sigma} + (p_2 - p_1)_\sigma \delta_{\nu\mu}] \delta(p_1 + p_2 + p_3)$.
- The $\bar{c}Ac$ -vertex: $\Gamma_{\bar{c}^a A_\mu^b c^c}(-p_1, -p_2, -p_3) = i g f^{abc} p_{1,\mu} \delta(p_1 + p_2 + p_3)$.
- The $AAAA$ -vertex: $\Gamma_{A_\mu^a A_\nu^b A_\rho^c A_\sigma^d}(-p_1, -p_2, -p_3, -p_4) = g^2 [f^{eab} f^{ecd} (\delta_{\mu\sigma} \delta_{\nu\rho} - \delta_{\mu\rho} \delta_{\nu\sigma}) + f^{eac} f^{ebd} (\delta_{\mu\sigma} \delta_{\nu\rho} - \delta_{\mu\nu} \delta_{\rho\sigma}) + f^{ead} f^{ebc} (\delta_{\mu\rho} \delta_{\nu\sigma} - \delta_{\mu\nu} \delta_{\rho\sigma})] \delta(p_1 + p_2 + p_3 + p_4)$.
- The $AAhh$ -vertex: $\Gamma_{A_\mu^a A_\nu^b h h}(-p_1, -p_2, -p_3, -p_4) = -\frac{1}{2} g^2 \delta^{ab} \delta_{\mu\nu}$.
- The $AA\rho\rho$ -vertex: $\Gamma_{A_\mu^a A_\nu^b \rho^c \rho^d}(-p_1, -p_2, -p_3, -p_4) = -\frac{1}{2} g^2 \delta_{\mu\nu} \delta^{ab} \delta^{cd}$.

Appendix B: Custodial symmetry

The custodial symmetry given in Sect. 2.2 is a result of the fact that the unbroken action is invariant under an $SU(2)_{\text{gauge}} \times SU(2)_{\text{global}}$ symmetry. This can be seen by writing Φ in the form of a bi-doublet [77]

$$\Phi = \begin{pmatrix} \phi^{0*} & \phi^+ \\ -\phi^{+*} & \phi^0 \end{pmatrix}. \tag{B1}$$

Clearly, the action,

$$\mathcal{L}_\Phi = \frac{1}{2} \text{Tr} (\mathcal{D}_\mu \Phi)^\dagger (\mathcal{D}_\mu \Phi) - \frac{\lambda}{4} (\text{Tr} \Phi^\dagger \Phi - v^2)^2, \tag{B2}$$

is invariant under the $SU(2)_{\text{gauge}} \times SU(2)_{\text{global}}$ transformation

$$\begin{aligned} \Phi &\rightarrow U(x)\Phi M^{-1}, \\ A_\mu &\rightarrow U(x)A_\mu U^{-1}(x) + \frac{i}{g} U(x)\partial_\mu U^{-1}(x), \end{aligned} \tag{B3}$$

with M an arbitrary x -independent matrix from $SU(2)_{\text{global}}$. In the bidoublet notation, the expansion in Eq. (8) becomes

$$\Phi = (h + v)\mathbf{1} + i\rho^a \tau^a, \tag{B4}$$

so the vev $\langle \Phi \rangle$ is not invariant under the transformation (B3). However, it is invariant under the global diagonal $SU(2) \times SU(2)$ subgroup corresponding to $U(x) = M$. This is the custodial symmetry, given in infinitesimal form in Eq. (20).

Appendix C: Elementary propagators in the R_ξ -gauge

Here we will calculate the one-loop corrections to the Higgs and gauge field propagator. This requires the calculation⁴ of the Feynman diagrams as shown in Figs. 8 and 9. To shorten the intermediate expressions, we will use the following functions:

$$\begin{aligned} \eta(m_1, m_2) &\equiv \frac{1}{(4\pi)^{d/2}} \Gamma\left(2 - \frac{d}{2}\right) \int_0^1 dx \left(p^2 x(1-x) \right. \\ &\quad \left. + x m_1 + (1-x) m_2 \right)^{d/2-2}, \\ \chi(m_1) &\equiv \frac{1}{(4\pi)^{d/2}} \Gamma\left(1 - \frac{d}{2}\right) m_1^{d/2-1}. \end{aligned} \tag{C1}$$

Notice that the last four diagrams for both particles are zero for $\langle h \rangle = 0$. In fact, including these diagrams has the same effect as making a shift in the vev of the scalar field Φ to demand $\langle h \rangle = 0$, see the Appendix of [23] for the technical details. In the context of the FMS operators, we found it more convenient to expand around the (classical) v that is gauge invariant, and thus to include the tadpoles. Expanding the FMS operator around the quantum corrected vev would lead to cancellations in that quantum vev coming from the propagator loop corrections to render it gauge invariant again, indeed the minimum of the quantum corrected effective Higgs potential is not gauge invariant itself.

a. Higgs propagator

The first diagrams contributing to the Higgs self-energy are of the snail type, renormalizing the masses of the internal fields. The Higgs boson snail (first diagram in the first line of Fig. 8):

$$\Gamma_{hh,1}(p^2) = -\frac{3\lambda\chi(m_h^2)}{2(m_h^2 + p^2)^2}, \tag{C2}$$

the Goldstone boson snail (second diagram in the first line of Fig. 8):

$$\Gamma_{hh,2}(p^2) = -\frac{3\lambda\chi(m^2\xi)}{2(m_h^2 + p^2)^2}, \tag{C3}$$

⁴ We have used from [78] the technique of modifying integrals into “master integrals” without numerators.

and the gauge field snail (third diagram in the first line of Fig. 8):

$$\Gamma_{hh,3}(p^2) = -\frac{3(d-1)g^2\chi(m^2)}{4(m_h^2 + p^2)^2} - \frac{3g^2\xi\chi(m^2\xi)}{4(m_h^2 + p^2)^2}. \tag{C4}$$

Next, we meet a couple of sunset diagrams. The Higgs boson sunset (fourth diagram in the first line of Fig. 8):

$$\Gamma_{hh,4}(p^2) = \frac{9\lambda^2 v^2 \eta(m_h^2, m_h^2)}{2(m_h^2 + p^2)^2}, \tag{C5}$$

the gauge field sunset (first diagram in the second line of Fig. 8):

$$\begin{aligned} \Gamma_{hh,5}(p^2) &= \frac{3g^2\eta(m^2, m^2)(4(d-1)m^4 + 4m^2p^2 + p^4)}{8m^2(m_h^2 + p^2)^2} \\ &\quad + \frac{3g^2(2m^2\xi + p^2)^2\eta(m^2\xi, m^2\xi)}{8m^2(m_h^2 + p^2)^2} \\ &\quad - \frac{3g^2(m^4(\xi-1)^2 + 2m^2\xi p^2 + 2m^2p^2 + p^4)\eta(m^2, m^2\xi)}{4m^2(m_h^2 + p^2)^2} \\ &\quad + \frac{3g^2(\xi-1)\chi(m^2)}{4(m_h^2 + p^2)^2} \\ &\quad - \frac{3g^2(\xi-1)\chi(m^2\xi)}{4(m_h^2 + p^2)^2}, \end{aligned} \tag{C6}$$

the ghost sunset (second diagram in the second line of Fig. 8):

$$\Gamma_{hh,6}(p^2) = -\frac{3g^2 m^2 \xi^2 \eta(m^2 \xi, m^2 \xi)}{4(m_h^2 + p^2)^2}, \tag{C7}$$

the Goldstone boson sunset (third diagram in the second line of Fig. 8):

$$\Gamma_{hh,7}(p^2) = \frac{3\lambda^2 v^2 \eta(m^2 \xi, m^2 \xi)}{2(m_h^2 + p^2)^2}, \tag{C8}$$

and a mixed Goldstone-gauge sunset (fourth diagram in the second line of Fig. 8):

$$\begin{aligned} \Gamma_{hh,8}(p^2) &= \frac{3g^2\left((m^2(\xi-1) + p^2)^2 + 4m^2p^2\right)\eta(m^2, m^2\xi)}{4m^2(m_h^2 + p^2)^2} \\ &\quad - \frac{3g^2(m^2\xi + p^2)^2\eta(m^2\xi, m^2\xi)}{4m^2(m_h^2 + p^2)^2} \\ &\quad + \frac{3g^2\chi(m^2\xi)(m^2(2\xi-1) + p^2)}{4m^2(m_h^2 + p^2)^2} \\ &\quad - \frac{3g^2\chi(m^2)(m^2(\xi-1) + p^2)}{4m^2(m_h^2 + p^2)^2}. \end{aligned} \tag{C9}$$

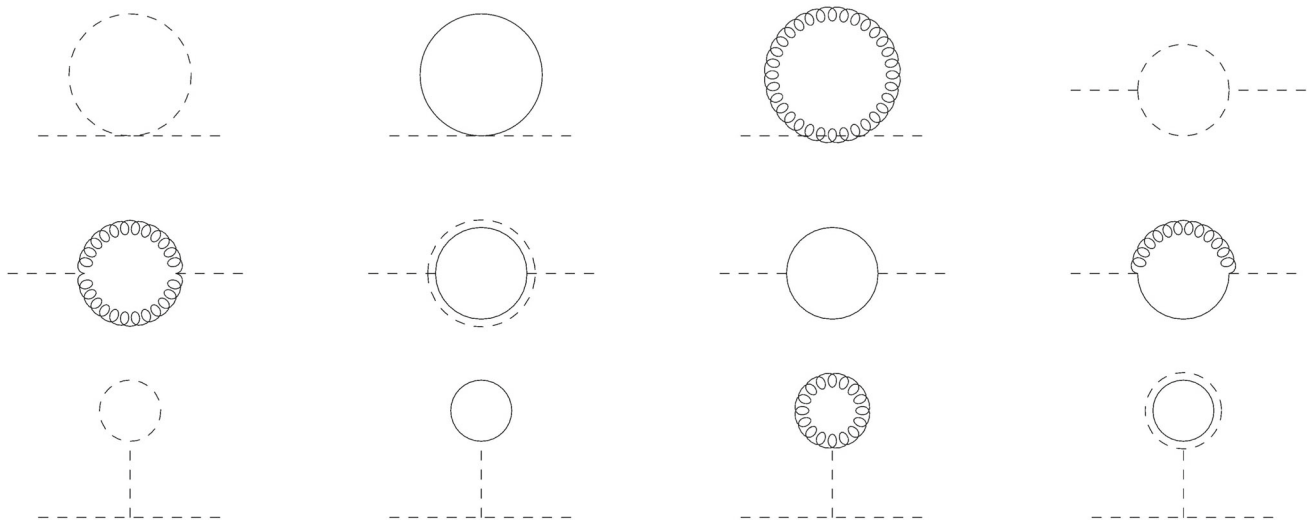


Fig. 8 One-loop contributions to the propagator $\langle h(p)h(-p) \rangle$. Curly lines represent the gauge field, dashed lines the Higgs field, solid lines the Goldstone boson and double lines the ghost field

Finally, we have the tadpole diagrams. The Higgs tadpole (first diagram on the third line of Fig. 8):

$$\Gamma_{hh,9}(p^2) = \frac{9\lambda^2 v^2 \chi(m_h^2)}{2m_h^2 (m_h^2 + p^2)^2}, \tag{C10}$$

the gauge tadpole (second diagram on the third line of Fig. 8):

$$\Gamma_{hh,10}(p^2) = \frac{9g\lambda m v ((d-1)\chi(m^2) + \xi\chi(m^2\xi))}{2m_h^2 (m_h^2 + p^2)^2}, \tag{C11}$$

the Goldstone boson tadpole (third diagram on the third line of Fig. 8):

$$\Gamma_{hh,11}(p^2) = \frac{9\lambda^2 v^2 \chi(m^2\xi)}{2m_h^2 (m_h^2 + p^2)^2}, \tag{C12}$$

the ghost tadpole (fourth diagram on the third line of Fig. 8):

$$\Gamma_{hh,12}(p^2) = -\frac{9g\lambda m \xi v \chi(m^2\xi)}{2m_h^2}. \tag{C13}$$

Putting together Eqs. (C2)–(C13) we find the Higgs up to first order in \hbar

$$\begin{aligned} \langle h(x)h(y) \rangle &= \frac{1}{p^2 + m_h^2} \\ &+ g^2 \left\{ \frac{3(4(d-1)m^4 + 4m^2 p^2 + p^4)}{8m^2} \eta(m^2, m^2) \right. \\ &+ \frac{9m_h^4}{8m^2} \eta(m_h^2, m_h^2) + \frac{3(m_h^4 - p^4)}{8m^2} \eta(m^2\xi, m^2\xi) \\ &+ \left. \frac{(6(d-1)m^2 - 3p^2)}{4m^2} \chi(m^2) \right\} \end{aligned}$$

$$\left. + \frac{3(m_h^2 + p^2)}{4m^2} \chi(m^2\xi) + \frac{3m_h^2}{4m^2} \chi(m_h^2) \right\} \frac{1}{(p^2 + m_h^2)^2}. \tag{C14}$$

b. Gauge field propagator

The first diagram contributing to transverse part of the gauge field self-energy is the gauge field snail (first diagram in the first line of Fig. 9) and gives a contribution:

$$\begin{aligned} \Pi_{AA^T,1}(p^2) &= \frac{2g^2(p^2 - d(d^2 - 3d + 3)p^2)\chi(m^2)}{(d-1)dp^2(m^2 + p^2)^2} \\ &- \frac{2g^2\xi((d-2)dp^2 + p^2)\chi(m^2\xi)}{(d-1)dp^2(m^2 + p^2)^2}. \tag{C15} \end{aligned}$$

The second diagram is the Goldstone boson snail (second diagram in the first line of Fig. 9):

$$\Pi_{AA^T,2}(p^2) = -\frac{3g^2\chi(m^2\xi)}{4(m^2 + p^2)^2}. \tag{C16}$$

The third diagram is the Higgs boson snail (third diagram in the first line of Fig. 9):

$$\Pi_{AA^T,3}(p^2) = -\frac{g^2\chi(m_h^2)}{4(m^2 + p^2)^2}. \tag{C17}$$

The fourth diagram is the gauge field sunrise (fourth diagram in the first line of Fig. 9):

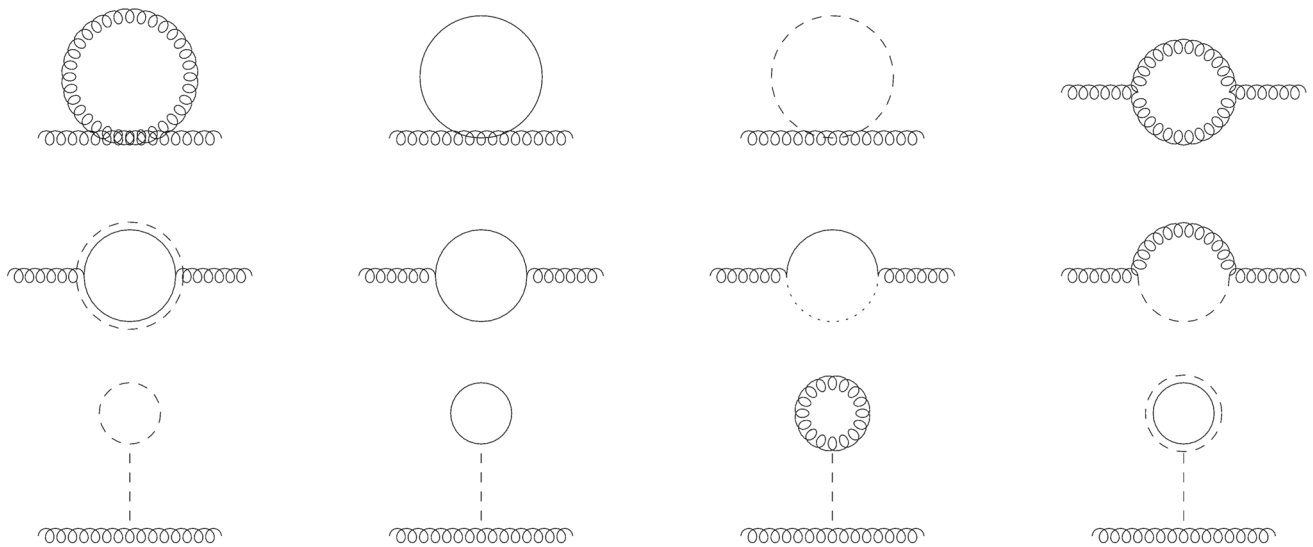


Fig. 9 Contributions to the one-loop gauge field self-energy

$$\begin{aligned} \Pi_{AA^T,4}(p^2) = g^2 & \left\{ \frac{\eta(m^2, m^2\xi) (2m^2p^2(-2d + \xi + 3) + m^4(\xi - 1)^2 + p^4)}{2(d - 1)m^4p^2} \right. \\ & - \frac{(4m^2 + p^2) \eta(m^2, m^2) (4(d - 1)m^4 + 4(3 - 2d)m^2p^2 + p^4)}{4(d - 1)m^4(m^2 + p^2)^2} - \frac{(4m^2\xi p^4 + p^6) \eta(m^2\xi, m^2\xi)}{4(d - 1)m^4(m^2 + p^2)^2} \\ & + \frac{\chi(m^2\xi) (4d^2(m^2(\xi + 1)p^2 + p^4) + d(m^4(\xi - 1) - m^2(6\xi + 7)p^2 + (\xi - 7)p^4) + 4m^2\xi p^2)}{2(d - 1)dm^2p^2(m^2 + p^2)^2} \\ & \left. - \frac{\chi(m^2) (4d^2p^4 + d(m^4(\xi - 1) + m^2(2\xi - 5)p^2 + (\xi - 7)p^4) + 4m^2p^2)}{2(d - 1)dm^2p^2(m^2 + p^2)^2} \right\}. \end{aligned} \tag{C18}$$

The fifth diagram is the ghost sunrise (first diagram in the second line of Fig. 9):

$$\begin{aligned} \Pi_{AA^T,5}(p^2) = g^2 & \left\{ \eta(m^2\xi, m^2\xi) \left(\frac{2m^2\xi}{(d - 1)(m^2 + p^2)^2} \right. \right. \\ & \left. \left. + \frac{p^2}{2(d - 1)(m^2 + p^2)^2} \right) - \frac{\chi(m^2\xi)}{(d - 1)(m^2 + p^2)^2} \right\}. \end{aligned} \tag{C19}$$

The sixth diagram is the Goldstone sunrise (second diagram in the second line of Fig. 9):

$$\begin{aligned} \Pi_{AA^T,6}(p^2) & = g^2 \left\{ \eta(m^2\xi, m^2\xi) \left(-\frac{m^2\xi}{(d - 1)(m^2 + p^2)^2} \right. \right. \\ & \left. \left. - \frac{p^2}{4(d - 1)(m^2 + p^2)^2} \right) + \frac{\chi(m^2\xi)}{2(d - 1)(m^2 + p^2)^2} \right\}. \end{aligned} \tag{C20}$$

The seventh diagram is the mixed Goldstone-Higgs sunrise (third diagram in the third line of Fig. 9):

$$\begin{aligned} \Pi_{AA^T,7}(p^2) & = g^2 \left\{ -\frac{\left((-m_h^2 + m^2\xi + p^2)^2 + 4m_h^2p^2 \right) \eta(m_h^2, m^2\xi)}{4(d - 1)p^2(m^2 + p^2)^2} \right. \\ & + \frac{\chi(m_h^2) (-m_h^2 + m^2\xi + p^2)}{4(d - 1)p^2(m^2 + p^2)^2} \\ & \left. + \frac{\chi(m^2\xi) (m_h^2 - m^2\xi + p^2)}{4(d - 1)p^2(m^2 + p^2)^2} \right\}. \end{aligned} \tag{C21}$$

The eighth diagram is the mixed Higgs-gauge field sunrise (fourth diagram in the second line of Fig. 9):

$$\Pi_{AA^T,8}(p^2)$$

$$\begin{aligned}
 &= g^2 \int_0^1 dx \frac{\left((m_h^2 - m^2 \xi + p^2)^2 + 4m^2 \xi p^2 \right) \eta(m_h^2, m^2 \xi)}{4(d-1)p^2(m^2 + p^2)^2} \\
 &\quad - \frac{\eta(m^2, m_h^2) \left((m_h^2 - m^2 + p^2)^2 - 4(d-2)m^2 p^2 \right)}{4(d-1)p^2(m^2 + p^2)^2} \\
 &\quad - \frac{m^2(\xi - 1)\chi(m_h^2)}{4(d-1)p^2(m^2 + p^2)^2} - \frac{\chi(m^2 \xi)(m_h^2 - m^2 \xi + p^2)}{4(d-1)p^2(m^2 + p^2)^2} \\
 &\quad + \frac{\chi(m^2)(m_h^2 - m^2 + p^2)}{4(d-1)p^2(m^2 + p^2)^2}. \tag{C22}
 \end{aligned}$$

Finally, we have four tadpole diagrams. The Higgs boson tadpole (first diagram of the third line in Fig. 9):

$$\Pi_{AA^T,5}(p^2) = \frac{3gm\chi(m_h^2)}{2v(m^2 + p^2)^2}, \tag{C23}$$

the Goldstone boson tadpole (second diagram of the last line in Fig. 9):

$$\Pi_{AA^T,6}(p^2) = \frac{3g\lambda mv\chi(m^2 \xi)}{2m_h^2(m^2 + p^2)^2}. \tag{C24}$$

The gauge field tadpole (third diagram of the last line in Fig. 9):

$$\Pi_{AA^T,7}(p^2) = \frac{3(d-1)g^2 m^2 \chi(m^2)}{2m_h^2(m^2 + p^2)^2} + \frac{3g^2 m^2 \xi \chi(m^2 \xi)}{2m_h^2(m^2 + p^2)^2} \tag{C25}$$

and finally, the ghost tadpole (fourth diagram of the last line in Fig. 9):

$$\Gamma_{AA^T,8}(p^2) = -\frac{3g^2 m^2 \xi \chi(m^2 \xi)}{2m_h^2(m^2 + p^2)^2}. \tag{C26}$$

Combining all these contributions (C15)–(C26), we find the total one-loop correction to the gauge field self-energy

$$\begin{aligned}
 \langle A_\mu^a(p) A_\nu^b(p) \rangle^T &= \frac{\delta^{ab}}{p^2 + m^2} + \delta^{ab} g^2 \left\{ -\frac{(2(3-2d)m^2 p^2 + m_h^4 - 2m_h^2(m^2 - p^2) + m^4 + p^4)}{4(d-1)p^2} \eta(m^2, m_h^2) \right. \\
 &\quad + \frac{(m^2 + p^2)^2 (2m^2 p^2(-2d + \xi + 3) + m^4(\xi - 1)^2 + p^4)}{2(d-1)m^4 p^2} \eta(m^2, m^2 \xi) \\
 &\quad + \frac{(m^4 - p^4)(4m^2 \xi + p^2)}{4(d-1)m^4} \eta(m^2 \xi, m^2 \xi) - \frac{(4m^2 + p^2)(4(d-1)m^4 + 4(3-2d)m^2 p^2 + p^4)}{4(d-1)m^4} \eta(m^2, m^2) \\
 &\quad + \frac{(m_h^2(-m^2 p^2(8d^2 - 24d + 4\xi + 13) - 2p^4(4d + \xi - 7) + m^4(1 - 2\xi)) + 6(d-1)^2 m^4 p^2 + m_h^4 m^2)}{4(d-1)m_h^2 m^2 p^2} \chi(m^2) \\
 &\quad - \frac{((d-2)p^2 + m_h^2 - m^2)}{4(d-1)p^2} \chi(m_h^2) + \frac{(m^2 p^2(5d + 4\xi - 13) + 2p^4(4d + \xi - 7) + 2m^4(\xi - 1))}{4(d-1)m^2 p^2} \chi(m^2 \xi) \\
 &\quad \left. + \frac{3}{4} \chi(m_h^2) + \frac{3}{4} \chi(m^2 \xi) \right\} \frac{1}{(p^2 + m^2)^2}. \tag{C27}
 \end{aligned}$$

Appendix D: Contributions to $\langle O(p)O(-p) \rangle$ in the R_ξ -gauge

The diagrams which contribute to the correlation function $\langle O(p)O(-p) \rangle$ are depicted in Fig. 10. The first term (first box in Fig. 10) is v^2 times the one-loop correction to the Higgs propagator, given in Eq. (C14). The second term (second box in Fig. 10) is

$$v \langle h(p)(\rho^a \rho^a)(-p) \rangle = -3 \frac{m_h^2 \eta(m^2 \xi, m^2 \xi)}{m_h^2 + p^2}. \tag{D1}$$

The third term (third box in Fig. 10) is

$$\begin{aligned}
 v \langle h(p)h^2(-p) \rangle &= -\frac{3m_h^2 \eta(m_h^2, m_h^2)}{m_h^2 + p^2} - \frac{3\chi(m_h^2)}{m_h^2 + p^2} - \frac{\chi(m^2 \xi)}{m_h^2 + p^2} \\
 &\quad - \frac{2(d-1)m^2 \chi(m^2)}{m_h^2(m_h^2 + p^2)} - \frac{2m^2 \xi \chi(m^2 \xi)}{m_h^2(m_h^2 + p^2)} \\
 &\quad + \frac{2m^2 \xi \chi(m^2 \xi)}{m_h^2(m_h^2 + p^2)}. \tag{D2}
 \end{aligned}$$

The fourth term (fourth box in Fig. 10) is

$$\langle m_h^2(p)m_h^2(-p) \rangle = \frac{1}{2} \eta(m_h^2, m_h^2). \tag{D3}$$

The fifth term (fifth box in Fig. 10) is

$$\langle (\rho^a \rho^a)(p)(\rho^b \rho^b)(-p) \rangle = \frac{3}{2} \eta(\xi m^2, \xi m^2) \tag{D4}$$

and together these terms give the correlation function of the scalar composite operator $O(p)$ up to first order in \hbar

$$\begin{aligned}
 \langle O(p)O(-p) \rangle &= \frac{v^2}{p^2 + m_h^2} + \left\{ \frac{3}{2} \eta(m^2, m^2) (4(d-1)m^4 \right.
 \end{aligned}$$

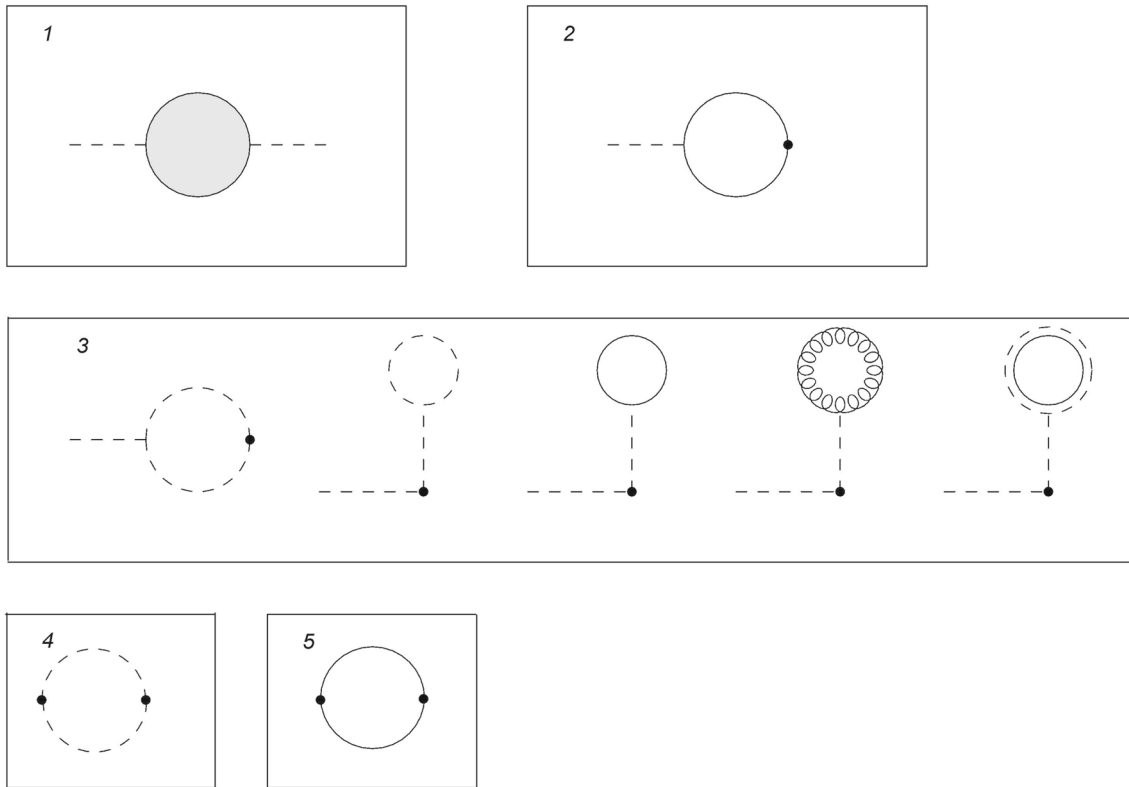


Fig. 10 One-loop contributions for the propagator $\langle O(x)O(y) \rangle$. Curly lines represent the gauge field, dashed lines the Higgs field, solid lines the Goldstone boson and double lines the ghost field. The \bullet indicates the insertion of a composite operator

$$\begin{aligned}
 &+4m^2 p^2 + p^4) + \frac{1}{2}(p^2 - 2m_h^2)^2 \eta(m_h^2, m_h^2) \\
 &- \frac{3p^2 \chi(m^2)(2(d-1)m^2 + m_h^2)}{m_h^2} - 3p^2 \chi(m_h^2) \Big\} \\
 &\times \frac{1}{(p^2 + m_h^2)^2}. \tag{D5}
 \end{aligned}$$

Appendix E: Contributions to $\langle R_\mu^a(p)R_\nu^a(-p) \rangle$ in the R_ξ -gauge

The diagrams which contribute to the correlation function $\langle R_\mu^a(p)R_\nu^a(-p) \rangle$ are depicted in Fig. 11. The first term (first box in Fig. 11) is $\frac{1}{16}g^2v^4$ times the one-loop corrected function, given by Eq. (C27). The second term (second box in Fig. 11) is

$$\begin{aligned}
 &-\langle \rho^a(p) \partial_\mu h(p), \partial_\nu \rho^a(-p) h(-p) \rangle \\
 &= \frac{3}{4(d-1)p^2} \left\{ \chi(m^2 \xi) (m_h^2 + p^2 - m^2 \xi) \right. \\
 &\quad - \left(4m_h^2 p^2 + (-m_h^2 + m^2 \xi + p^2)^2 \right) \eta(m_h^2, m^2 \xi) \\
 &\quad \left. - \chi(m_h^2) (m_h^2 - m^2 \xi - p^2) \right\} \mathcal{P}_{\mu\nu}(p). \tag{E1}
 \end{aligned}$$

The third term (third box in Fig. 11) is

$$\begin{aligned}
 &-\frac{1}{2} \langle \rho^a(x) \partial_\mu \rho^b(x), \partial_\nu \rho^a(y) \rho^b(y) \rangle \\
 &= \left\{ \frac{3\chi(m^2 \xi)}{2(d-1)} - \frac{3(4m^2 \xi + p^2) \eta(m^2 \xi, m^2 \xi)}{4(d-1)} \right\} \mathcal{P}_{\mu\nu}(p). \tag{E2}
 \end{aligned}$$

The fourth term (fourth box in Fig. 11) is

$$\begin{aligned}
 &\frac{1}{4}g^2v^3 \langle A_\mu^a(x), A_\nu^a(y) h(y) \rangle \\
 &= \left\{ -\frac{3m^2 \left((-m_h^2 + m^2 \xi + p^2)^2 + 4m_h^2 p^2 \right) \eta(m_h^2, m^2 \xi)}{2(d-1)p^2(m^2 + p^2)} \right. \\
 &\quad + \frac{3m^2 \eta(m^2, m_h^2) \left(4p^2(m_h^2 - (d-1)m^2) + (-m_h^2 + m^2 + p^2)^2 \right)}{2(d-1)p^2(m^2 + p^2)} \\
 &\quad + \frac{3m^2 \chi(m^2 \xi) \left(\frac{m_h^2 - m^2 \xi + p^2}{(d-1)p^2} - 3 \right)}{2(m^2 + p^2)} \\
 &\quad + \frac{3m^4 \chi(m_h^2) \left(\frac{\xi - 1}{(d-1)p^2} - \frac{3}{m^2} \right)}{2(m^2 + p^2)} \\
 &\quad \left. - \frac{3m^2 \chi(m^2) \left(6(d-1)m^2 p^2 + m_h^4 + m_h^2(p^2 - m^2) \right)}{2(d-1)m_h^2 p^2(m^2 + p^2)} \right\} \mathcal{P}_{\mu\nu}(p). \tag{E3}
 \end{aligned}$$

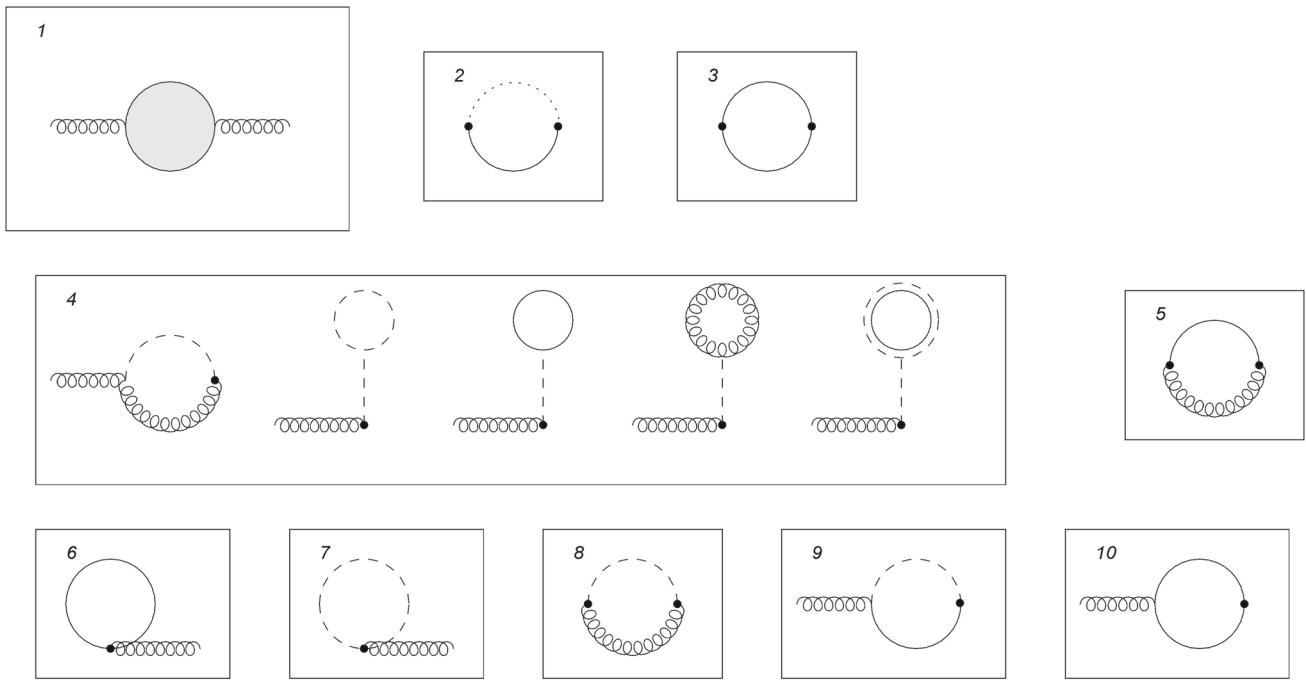


Fig. 11 One-loop contributions for the propagator $\langle R_\mu^a(x) R_\nu^a(y) \rangle$ in the unitary gauge. Curly lines represent the gauge field, dashed lines the Higgs field, solid lines the Goldstone boson and double lines the ghost field. The \bullet indicates the insertion of a composite operator

The fifth term (fifth box in Fig. 11) is

$$\begin{aligned} & \frac{1}{6} g^2 v^2 \langle \rho^a(x) A_\mu^b(x), \rho^a(y) A_\nu^b(y) \rangle \\ &= \left\{ -\frac{3 \left((m^2(\xi - 1) + p^2)^2 - 4(d - 2)m^2 p^2 \right) \eta(m^2, m^2\xi)}{2(d - 1)p^2} \right. \\ & \quad + \frac{3(4m^2\xi + p^2) \eta(m^2\xi, m^2\xi)}{2(d - 1)} + \frac{3\chi(m^2)(m^2(\xi - 1) + p^2)}{2(d - 1)p^2} \\ & \quad \left. - \frac{3\chi(m^2\xi)(m^2(\xi - 1) + p^2)}{2(d - 1)p^2} \right\} \mathcal{P}_{\mu\nu}(p) \end{aligned} \tag{E4}$$

The sixth term is

$$\begin{aligned} & -\frac{1}{24} g^2 v^2 \langle \rho^a(x) \rho^a(x) A_\mu^b(x), A^b(y) \rangle \\ &= -\frac{3g^2 v^2 \chi(\xi m^2)}{8(m^2 + p^2)} \mathcal{P}_{\mu\nu}(p). \end{aligned} \tag{E5}$$

The seventh term (seventh box in Fig. 11) is

$$\frac{1}{8} g^2 v^2 \langle h(x) h(x) A_\mu^a(x), A_\nu^a(y) \rangle = \frac{3g^2 v^2 \chi(m_h^2)}{8(m^2 + p^2)} \mathcal{P}_{\mu\nu}(p). \tag{E6}$$

The eighth term (eighth box in Fig. 11) is

$$\begin{aligned} & \frac{1}{4} g^2 v^2 \langle h(x) A_\mu^a(x), h(y) A_\nu^a(y) \rangle \\ &= 3m^2 \left\{ \frac{\left((-m_h^2 + m^2\xi + p^2)^2 + 4m_h^2 p^2 \right) \eta(m_h^2, m^2\xi)}{4(d - 1)m^2 p^2} \right. \end{aligned}$$

$$\begin{aligned} & \left. - \frac{\eta(m^2, m_h^2) \left(4p^2(m_h^2 - (d - 1)m^2) + (-m_h^2 + m^2 + p^2)^2 \right)}{4(d - 1)m^2 p^2} \right. \\ & \quad + \frac{\chi(m^2\xi)(-m_h^2 + m^2\xi - p^2)}{4(d - 1)m^2 p^2} + \frac{\chi(m^2)(m_h^2 - m^2 + p^2)}{4(d - 1)m^2 p^2} \\ & \quad \left. - \frac{(\xi - 1)\chi(m_h^2)}{4(d - 1)p^2} \right\} \mathcal{P}_{\mu\nu}(p). \end{aligned} \tag{E7}$$

The ninth term (ninth box in Fig. 11) is

$$\begin{aligned} & \frac{1}{2} g v^2 \langle \partial_\mu h(x) \rho^a(x), A_\nu^a(y) \rangle \\ &= -\frac{3}{2} g^2 v^2 \left\{ -\frac{\left((-m_h^2 + m^2\xi + p^2)^2 + 4m_h^2 p^2 \right) \eta(m_h^2, m^2\xi)}{4(d - 1)p^2(m^2 + p^2)} \right. \\ & \quad + \frac{\chi(m_h^2)(-m_h^2 + m^2\xi + p^2)}{4(d - 1)p^2(m^2 + p^2)} \\ & \quad \left. + \frac{\chi(m^2\xi)(m_h^2 - m^2\xi + p^2)}{4(d - 1)p^2(m^2 + p^2)} \right\} \mathcal{P}_{\mu\nu}(p). \end{aligned} \tag{E8}$$

The tenth term (tenth box in Fig. 11) is

$$\begin{aligned} & -\frac{1}{4} g v^2 \varepsilon^{abc} \langle A^a(x), \rho^b \partial_\mu \rho^c \rangle \\ &= -\frac{3}{4} g^2 v^2 \left\{ \frac{(4m^2\xi p^2 + p^4) \eta(m^2\xi, m^2\xi)}{2(d - 1)p^2(m^2 + p^2)} \right. \\ & \quad \left. - \frac{\chi(m^2\xi)}{(d - 1)(m^2 + p^2)} \right\} \mathcal{P}_{\mu\nu}(p) \end{aligned} \tag{E9}$$

and together these terms give the transverse part of the correlation function of the scalar composite operator R_μ^a up to first order in \hbar

We used here that the surviving tree level propagators in the unitary gauge are

$$\begin{aligned} \langle R_\mu^a(x), R_\nu^a(y) \rangle^T &= \frac{3}{16} g^2 v^4 \frac{1}{p^2 + m^2} - 3 \left\{ - \frac{p^2 (2(3 - 2d)m^2 p^2 - 2m_h^2 (m^2 - p^2) + m_h^4 + m^4 + p^4)}{4(d - 1)} \eta(m^2, m_h^2) \right. \\ &\quad - \frac{(4m^2 + p^2) (4(d - 1)m^4 + 4(3 - 2d)m^2 p^2 + p^4)}{4(d - 1)} \eta(m^2, m^2) \\ &\quad + \frac{\chi(m^2) (m_h^2 (-8(d^2 - 3d + 2)m^4 + (15 - 8d)m^2 p^2 + 3p^4) - 6(d - 1)^2 m^4 (m^2 + 2p^2) + p^2 m_h^4)}{4(d - 1)m_h^2} \\ &\quad \left. + \frac{\chi(m_h^2) (-2(d - 1)m^4 + (5 - 4d)m^2 p^2 - p^2 m_h^2 + p^4)}{4(d - 1)} \right\} \frac{1}{(m^2 + p^2)^2}. \end{aligned} \tag{E10}$$

Appendix F: Fundamental Feynman integral

$$\begin{aligned} &\int_0^1 dx \ln \frac{p^2 x(1 - x) + xm_1^2 + (1 - x)m_2^2}{\mu^2} \\ &= -2 + \frac{1}{2p^2} \left\{ m_1^2 \ln \left(\frac{m_2^2}{m_1^2} \right) + m_2^2 \ln \left(\frac{m_1^2}{m_2^2} \right) + p^2 \ln \left(\frac{m_1^2 m_2^2}{\mu^4} \right) \right. \\ &\quad - 2\sqrt{-m_1^4 + 2m_1^2 m_2^2 - 2m_1^2 p^2 - m_2^4 - 2m_2^2 p^2 - p^4} \\ &\quad \times \tan^{-1} \left[\frac{-m_1^2 + m_2^2 - p^2}{\sqrt{-m_1^4 + 2m_1^2 (m_2^2 - p^2) - (m_2^2 + p^2)^2}} \right] \\ &\quad + 2\sqrt{-m_1^4 + 2m_1^2 m_2^2 - 2m_1^2 p^2 - m_2^4 - 2m_2^2 p^2 - p^4} \\ &\quad \left. \times \tan^{-1} \left[\frac{-m_1^2 + m_2^2 + p^2}{\sqrt{-m_1^4 + 2m_1^2 (m_2^2 - p^2) - (m_2^2 + p^2)^2}} \right] \right\}. \end{aligned} \tag{F1}$$

Appendix G: A digression on the unitary gauge

It is well-known that in the unitary gauge the unphysical fields, like the Goldstone and ghost fields, decouple, a feature which allows for a more direct link with the spectrum of the elementary excitations of the model. However, this gauge is known to be non-renormalizable. In fact, working directly with the elementary tree level propagators taken a priori in the unitary limit, i.e. $\xi \rightarrow \infty$, and following the steps of dimensional regularization, we find that the divergent part of the inverse Higgs propagator reads

$$G_{hh, \text{div}}^{-1}(p^2) = \frac{3g^2 (m_h^4 + 6m^2 p^2 + p^4)}{64\pi^2 m^2 \epsilon}. \tag{G1}$$

$$\begin{aligned} \langle A_\mu^a(p) A_\nu^b(-p) \rangle &= \frac{\delta^{ab}}{p^2 + m^2} \mathcal{P}_{\mu\nu}(p) \\ &\quad + \delta^{ab} \frac{1}{m^2} \mathcal{L}_{\mu\nu}(p) = \frac{\delta^{ab}}{p^2 + m^2} \left(\delta_{\mu\nu} + \frac{p_\mu p_\nu}{m^2} \right), \\ \langle h(p) h(-p) \rangle &= \frac{1}{p^2 + m_h^2} \end{aligned} \tag{G2}$$

with all other propagators, i.e. the Goldstone and Faddeev-Popov ghost propagators, vanishing. In expression (G1) we clearly see the presence of the term $\sim \frac{p^4}{\epsilon m^2}$, signalling the aforementioned issue of the non-renormalizability. In essence, this can be traced back to the tree level presence of $\frac{p_\mu p_\nu}{m^2}$, a non power-counting controllable term.

Nevertheless, it is interesting to observe that, if we remove the divergent part (G1) anyway, we obtain the spectral function as shown in Fig. 12. This spectral function is almost identical to that obtained for the composite operator $O(x)$, see Fig. 6.

For the inverse gauge field propagator, proceeding in the same way, we find the divergent part

$$\begin{aligned} G_{AA, \text{div}}^{-1}(p^2) &= \frac{1}{\epsilon} \left(- \frac{9g^2 m^4}{16\pi^2 m_h^2} - \frac{g^2 p^6}{96\pi^2 m^4} \right. \\ &\quad \left. + \frac{7g^2 p^4}{48\pi^2 m^2} + \frac{3g^2 m^2}{32\pi^2} + \frac{83g^2 p^2}{96\pi^2} - \frac{3\lambda m^2}{8\pi^2} \right) \end{aligned} \tag{G3}$$

which shows again the non-renormalizability of unitary gauge, through the terms $\sim \frac{p^6}{\epsilon m^4}$ and $\sim \frac{p^4}{\epsilon m^2}$. However, if we remove also here those terms by hand, we obtain the spectral function as shown in Fig. 13.

Apart from the by hand removal of the divergences in this unitary gauge exercise, the nice behaviour of the spectral

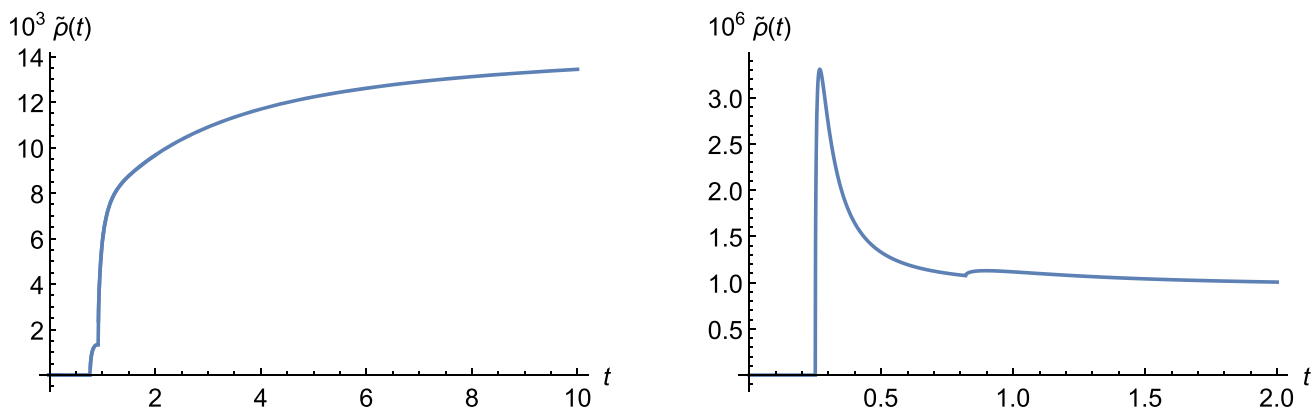


Fig. 12 Spectral function for the propagator $\langle h(p)h(-p) \rangle$ in the unitary gauge, with t given in unity of μ^2 , for the Region I (left) and Region II (right), with parameter values given in Table 1

densities for the Higgs and gauge field⁵ obtained by a direct use of the tree level propagators already taken in the unitary limit, $\xi \rightarrow \infty$, can be, to some extent, justified by the fact that we are working at the one-loop order in perturbation theory. Since overlapping divergences start from two-loop onward, we can easily figure out that the naive use of the elementary tree level propagators taken already in the unitary limit will run into severe non-renormalizability issues, making the removal of the (overlapping) divergent parts (G1), (G3) quite problematic beyond the current one-loop level.

Now for what concerns the composite operators, since $O(x)$ is BRST invariant, any choice for the gauge fixing should give the same expression for the correlation function $G_{OO}(p^2)$. So again using the unitary gauge, Eq. (44) simplifies to

$$\langle O(x)O(y) \rangle_{\text{unitary}} = v^2 \langle h(x)h(y) \rangle_{\text{unitary}} + v \langle h(x)h(y)^2 \rangle_{\text{unitary}} + \frac{1}{4} \langle h(x)^2h(y)^2 \rangle_{\text{unitary}}, \quad (\text{G4})$$

with the consecutive terms displayed diagrammatically by the respective boxes in Fig. 14. Using dimensional regularization in the $\overline{\text{MS}}$ -scheme with $(d = 4 - \epsilon)$ and switching to momentum space, we find

$$\begin{aligned} v^2 \langle h(p)h(-p) \rangle_{\text{unitary}} &= \frac{3}{32\pi^2} \int_0^1 dx \left\{ \frac{1}{\epsilon} (2m_h^4 + 12m^2 p^2 + 2p^4) \right. \\ &+ 2m_h^4 \ln \left(\frac{m_h^2}{\mu^2} \right) + 2(6m^4 - m^2 p^2) \ln \left(\frac{m^2}{\mu^2} \right) \\ &- 3m_h^4 \ln \left(\frac{p^2(1-x)x + m_h^2}{\mu^2} \right) \\ &\left. - (12m^4 + 4m^2 p^2 + p^4) \ln \left(\frac{p^2(1-x)x + m^2}{\mu^2} \right) \right\} \end{aligned}$$

⁵ Notice that these dropped divergences do not contribute anyhow to the branch cut discontinuity and this spectral function.

$$-2m_h^4 + 2m^2(p^2 - 6m^2) \left\} \frac{1}{(m_h^2 + p^2)^2}, \quad (\text{G5})$$

$$\begin{aligned} v \langle h(p)h(-p)^2 \rangle_{\text{unitary}} &= \frac{3}{16\pi^2 m_h^2} \int_0^1 dx \left\{ \frac{12}{\epsilon} m^4 - 6m^4 \ln \left(\frac{m^2}{\mu^2} \right) - m_h^4 \ln \left(\frac{m_h^2}{\mu^2} \right) \right. \\ &\left. + m_h^4 \ln \left(\frac{m_h^2 + p^2(1-x)x}{\mu^2} \right) + m_h^4 + 2m^4 \right\} \frac{1}{(m_h^2 + p^2)}, \quad (\text{G6}) \end{aligned}$$

$$\begin{aligned} \frac{1}{4} \langle h(p)^2h(p)^2 \rangle_{\text{unitary}} &= \frac{1}{16\pi^2} \int_0^1 dx \left\{ \frac{1}{\epsilon} - \frac{1}{2} \ln \left(\frac{m_h^2 + p^2(1-x)x}{\mu^2} \right) \right\}. \quad (\text{G7}) \end{aligned}$$

Inserting now the unity

$$1 = (p^2 + m_h^2)/(p^2 + m_h^2) = ((p^2 + m_h^2)/(p^2 + m_h^2))^2, \quad (\text{G8})$$

we find indeed that the finite pieces of $\langle O(x)O(y) \rangle_{\text{unitary}}$ and $\langle O(x)O(y) \rangle_{R_\xi}$ do coincide, this is evidently related to the gauge invariance. From two-loop onward the overlapping divergences will show up again, requiring a fully renormalizable setup.

We can stretch the unitary gauge even a bit further, to also look at the vector correlator, $\langle R_\mu^a(p) R_\nu^a(-p) \rangle_{\text{unitary}}$. We find at one-loop order

$$\begin{aligned} \langle R_\mu^a(p) R_\nu^a(-p) \rangle &= \frac{1}{16} g^2 v^4 \langle A_\mu^a(p) A_\nu^a(-p) \rangle_{\text{unitary}} \\ &+ \frac{1}{4} g^2 v^3 \langle A_\mu^a(p) (A_\nu^a h)(-p) \rangle_{\text{unitary}} \\ &+ \frac{1}{8} g^2 v^2 \langle (h^2 A_\mu^a)(p) A_\nu^a(-p) \rangle_{\text{unitary}} \\ &+ \frac{1}{4} g^2 v^2 \langle (h A_\mu^a)(p) (h A_\nu^a)(-p) \rangle_{\text{unitary}} \quad (\text{G9}) \end{aligned}$$

with the consecutive terms displayed diagrammatically by the respective boxes in Fig. 15.

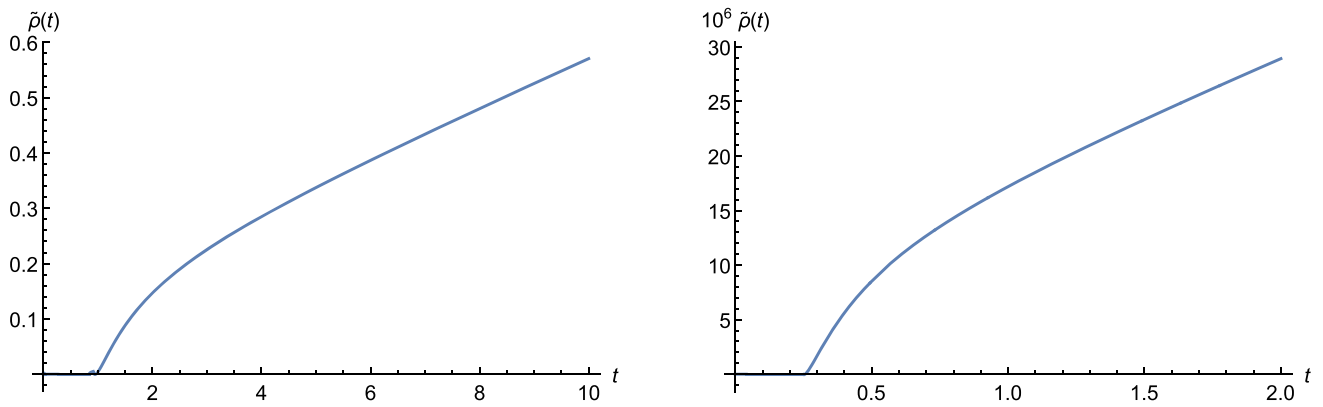


Fig. 13 Spectral function for the propagator $\langle A_\mu^a(p)A_\nu^b(-p) \rangle$ in the unitary gauge, with t given in unity of μ^2 , for the Region I (left) and Region II (right), with parameter values given in Table 1

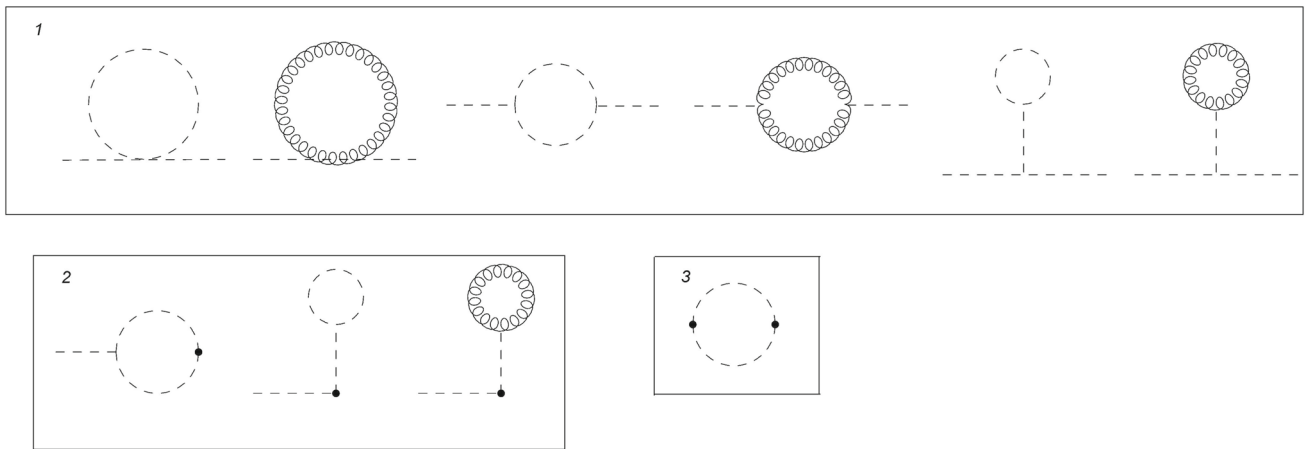


Fig. 14 One-loop contributions for the propagator $\langle O(x)O(y) \rangle$ in the unitary gauge. Curly lines represent the gauge field and dashed lines the Higgs field. The \bullet indicates the insertion of a composite operator

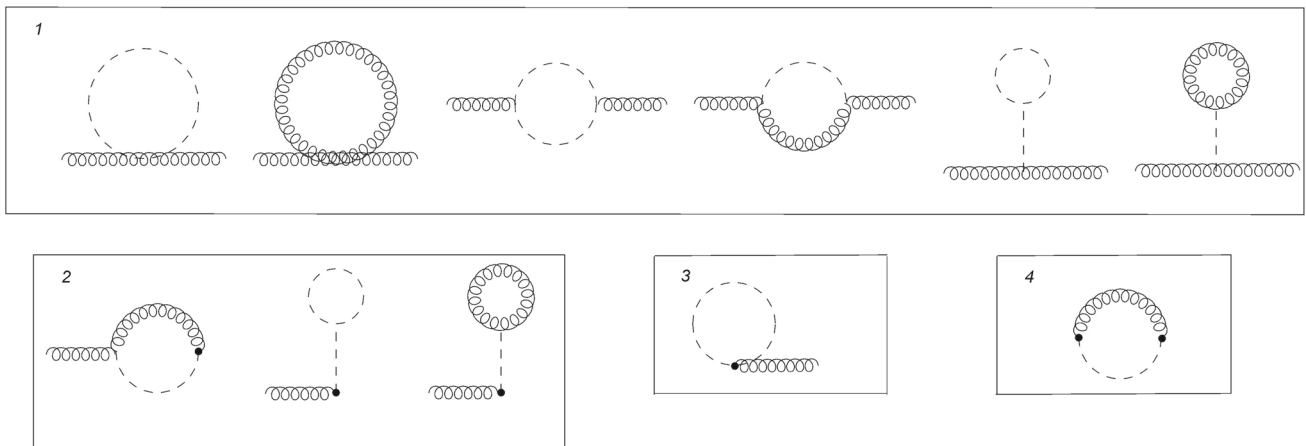


Fig. 15 One-loop contributions for the propagator $\langle R_\mu^a(x)R_\nu^a(y) \rangle$ in the unitary gauge. Curly lines represent the gauge field and dashed lines the Higgs field. The \bullet indicates the insertion of a composite operator

We find in momentum space

$$\begin{aligned} & \frac{1}{16} g^2 v^4 \langle A_\mu^a(p) A_\nu^a(-p) \rangle_{\text{unitary}} \\ &= \frac{g^4 v^4}{32(4\pi)^2} \int_0^1 dx \left\{ -\frac{1}{\epsilon} \frac{1}{6m^4 m_h^2} (9m^4 m_h^4 + m_h^2 (-9m^6 \right. \\ & \quad - 83m^4 p^2 - 14m^2 p^4 + p^6) + 54m^8) \\ & \quad + \frac{m_h^2}{2p^2} (-m_h^2 + m^2 + 7p^2) \ln \left(\frac{m_h^2}{\mu^2} \right) \\ & \quad + \frac{1}{2m^2 p^2 m_h^2} (m^4 m_h^4 - m_h^2 (m^6 + 47m^4 p^2 \\ & \quad + 16m^2 p^4 - 2p^6) + 54m^6 p^2) \ln \left(\frac{m^2}{\mu^2} \right) \\ & \quad + \frac{1}{2p^2} (-2m_h^2 (m^2 - p^2) + m_h^4 + m^4 \\ & \quad - 10m^2 p^2 + p^4) \ln \left(\frac{p^2(1-x)x + (1-x)m_h^2 + m^2 x}{\mu^2} \right) \\ & \quad + \frac{1}{2m^4} (4m^2 + p^2) (12m^4 - 20m^2 p^2 + p^4) \\ & \quad \times \ln \left(\frac{m^2 + p^2(1-x)x}{\mu^2} \right) \\ & \quad + \frac{1}{6m^4 p^2 m_h^2} (3m^4 m_h^6 - 3m_h^4 (2m^6 + 9m^4 p^2) \\ & \quad + m_h^2 (3m^8 - 9m^6 p^2 - 2m^4 p^4 - 26m^2 p^6 - 2p^8) \\ & \quad - 54m^8 p^2) \left. \right\} \frac{\mathcal{P}_{\mu\nu}(p)}{(p^2 + m^2)^2} + \frac{g^4 v^4}{32(4\pi)^2 m^4} \int_0^1 dx \left\{ \frac{1}{\epsilon} \frac{3}{m_h^2} \right. \\ & \quad \times (m_h^2 (3m^2 + p^2) - 3m_h^4 - 18m^4) \\ & \quad - \frac{3m^2}{2p^2 m_h^2} (m_h^2 (p^2 - m^2) + m_h^4 - 18m^2 p^2) \ln \left(\frac{m^2}{\mu^2} \right) \\ & \quad + \frac{3m_h^2}{2p^2} (m_h^2 - m^2 + 5p^2) \ln \left(\frac{m_h^2}{\mu^2} \right) \\ & \quad - \frac{3}{2p^2} ((m_h - m)^2 + p^2) ((m_h + m)^2 + p^2) \\ & \quad \times \ln \left(\frac{p^2(1-x)x + (1-x)m_h^2 + m^2 x}{\mu^2} \right) \\ & \quad - \frac{3}{2p^2 m_h^2} (m_h^4 (5p^2 - 2m^2) \\ & \quad \left. + m_h^2 (m^4 - m^2 p^2) + m_h^6 + 6m^4 p^2) \right\} \mathcal{L}_{\mu\nu}(p), \end{aligned}$$

$$\begin{aligned} & \frac{1}{4} g^2 v^3 \langle A_\mu^a(p) (A_\nu^a h)(-p) \rangle_{\text{unitary}} \\ &= \frac{1}{16\pi^2} \int_0^1 dx \left\{ \frac{1}{\epsilon} \frac{m^2}{m_h^2} (m_h^2 (p^2 - 9m^2) + 12m_h^4 + 54m^4) \right. \\ & \quad - \frac{m^2 m_h^2}{2p^2} (-m_h^2 + m^2 + 10p^2) \ln \left(\frac{m_h^2}{\mu^2} \right) \\ & \quad - \frac{m^4}{2p^2 m_h^2} (m_h^2 (p^2 - m^2) + m_h^4 + 54m^2 p^2) \ln \left(\frac{m^2}{\mu^2} \right) \\ & \quad \left. - \frac{m^2}{2p^2} (2p^2 (m_h^2 - 5m^2) + (m^2 - m_h^2)^2 + p^4) \right\} \end{aligned}$$

$$\begin{aligned} & \times \ln \left(\frac{p^2(1-x)x + (1-x)m_h^2 + xm^2}{\mu^2} \right) \\ & + \frac{m^2}{6p^2 m_h^2} (6m_h^4 (m^2 + 6p^2) \\ & + m_h^2 (-3m^4 + 9m^2 p^2 + 2p^4) \\ & - 3m_h^6 + 54m^4 p^2) \left. \right\} \frac{\mathcal{P}_{\mu\nu}(p)}{(m^2 + p^2)} \\ & + \frac{1}{16\pi^2} \int_0^1 dx \left\{ \frac{1}{\epsilon} \frac{3}{m_h^2} (-m_h^2 (3m^2 + p^2) + m_h^4 + 18m^4) \right. \\ & + \frac{3m^2}{2p^2 m_h^2} (m_h^2 (p^2 - m^2) + m_h^4 - 18m^2 p^2) \ln \left(\frac{m^2}{\mu^2} \right) \\ & - \frac{3m_h^2}{2p^2} (m_h^2 - m^2 + 3p^2) \ln \left(\frac{m_h^2}{\mu^2} \right) \\ & + \frac{3}{2p^2 m_h^2} (m_h^2 ((m - m_h)^2 + p^2) ((m_h + m)^2 + p^2)) \\ & \times \ln \left(\frac{p^2(1-x)x + (1-x)m_h^2 + xm^2}{\mu^2} \right) \\ & \left. + \frac{3}{2p^2 m_h^2} ((m_h^3 - m^2 m_h)^2 \right. \\ & \left. + p^2 (-m^2 m_h^2 + 3m_h^4 + 6m^4)) \right\} \mathcal{L}_{\mu\nu}(p), \tag{G10} \end{aligned}$$

$$\begin{aligned} & \frac{1}{8} g^2 v^2 \langle (h^2 A_\mu^a)(p) A_\nu^a(-p) \rangle_{\text{unitary}} \\ &= -\frac{3m_h^2 m^2}{32\pi^2} \int_0^1 dx \left\{ \frac{2}{\epsilon} - \ln \left(\frac{m_h^2}{\mu^2} \right) + 1 \right\} \\ & \times \left(\frac{1}{p^2 + m^2} \mathcal{P}_{\mu\nu}(p) + \frac{1}{m^2} \mathcal{L}_{\mu\nu}(p) \right), \tag{G11} \end{aligned}$$

$$\begin{aligned} & \frac{1}{4} g^2 v^2 \langle (h A_\mu^a)(p) (h A_\nu^a)(-p) \rangle_{\text{unitary}} \\ &= \frac{1}{32\pi^2} \int_0^1 dx \left\{ \frac{1}{\epsilon} (-3m_h^2 + 9m^2 - p^2) \right. \\ & + \frac{m_h^2}{2p^2} (m^2 + p^2 - m_h^2) \ln \left(\frac{m_h^2}{\mu^2} \right) \\ & + \frac{m^2}{2p^2} (m_h^2 - m^2 + p^2) \ln \left(\frac{m^2}{\mu^2} \right) \\ & + \frac{1}{2p^2} (2p^2 (m_h^2 - 5m^2) + (m^2 - m_h^2)^2 + p^4) \\ & \times \ln \left(\frac{p^2(1-x)x + (1-x)m_h^2 + xm^2}{\mu^2} \right) \\ & \left. + \frac{1}{6p^2} (3(m^2 - m_h^2)^2 - 9p^2 (m_h^2 + m^2) - 2p^4) \right\} \mathcal{P}_{\mu\nu}(p) \\ & + \frac{3}{32\pi^2} \int_0^1 dx \left\{ \frac{1}{\epsilon} (-m_h^2 + 3m^2 + p^2) \right. \\ & \left. + \frac{m^2}{2p^2} (-m_h^2 + m^2 - p^2) \ln \left(\frac{m^2}{\mu^2} \right) \right\} \end{aligned}$$

$$\begin{aligned}
& + \frac{m_h^2}{2p^2} (m_h^2 - m^2 + 3p^2) \ln \left(\frac{m_h^2}{\mu^2} \right) \\
& - \frac{1}{2p^2} ((m - m_h)^2 + p^2) ((m_h + m)^2 + p^2) \\
& \times \ln \left(\frac{p^2 x(1-x) + (1-x)m_h^2 + xm^2}{\mu^2} \right) \\
& - \frac{1}{2p^2} ((m^2 - m_h^2)^2 + 3p^2 m_h^2 - p^2 m^2) \left. \right\} \mathcal{L}_{\mu\nu}(p). \quad (\text{G12})
\end{aligned}$$

and putting everything together, also here we see that $\langle R_\mu^a(p) R_\nu^a(-p) \rangle_{\text{unitary}} = \langle R_\mu^a(p) R_\nu^a(-p) \rangle_{R_\xi}$ upon dropping the divergences.

References

- G. 't Hooft, C. Itzykson, A. Jaffe, H. Lehmann, P.K. Mitter, I.M. Singer, R. Stora, NATO Sci. Ser. B **59**, 1 (1980). <https://doi.org/10.1007/978-1-4684-7571-5>
- M.E. Peskin, D.V. Schroeder, An Introduction to Quantum Field Theory (Addison-Wesley, Reading, 1995). <https://doi.org/10.1063/1.2807734>. <http://www.slac.stanford.edu/~mpeskin/QFT.html>
- F. Jegerlehner, MYu. Kalmykov, O. Veretin, Nucl. Phys. B **641**, 285 (2002). [https://doi.org/10.1016/S0550-3213\(02\)00613-2](https://doi.org/10.1016/S0550-3213(02)00613-2). arXiv:hep-ph/0105304
- F. Jegerlehner, MYu. Kalmykov, O. Veretin, Nucl. Phys. B **658**, 49 (2003). [https://doi.org/10.1016/S0550-3213\(03\)00177-9](https://doi.org/10.1016/S0550-3213(03)00177-9). arXiv:hep-ph/0212319
- S.P. Martin, Phys. Rev. D **91**, 114003 (2015a). <https://doi.org/10.1103/PhysRevD.91.114003>. arXiv:1503.03782 [hep-ph]
- S.P. Martin, Phys. Rev. D **92**, 014026 (2015b). <https://doi.org/10.1103/PhysRevD.92.014026>. arXiv:1505.04833 [hep-ph]
- N.K. Nielsen, Nucl. Phys. B **101**, 173 (1975). [https://doi.org/10.1016/0550-3213\(75\)90301-6](https://doi.org/10.1016/0550-3213(75)90301-6)
- I. Aitchison, C. Fraser, Ann. Phys. **156**, 1 (1984). [https://doi.org/10.1016/0003-4916\(84\)90209-4](https://doi.org/10.1016/0003-4916(84)90209-4)
- O. Piguet, K. Sibold, Nucl. Phys. B **253**, 517 (1985). [https://doi.org/10.1016/0550-3213\(85\)90545-0](https://doi.org/10.1016/0550-3213(85)90545-0)
- P. Gambino, P.A. Grassi, F. Madricardo, Phys. Lett. B **454**, 98 (1999). [https://doi.org/10.1016/S0370-2693\(99\)00321-4](https://doi.org/10.1016/S0370-2693(99)00321-4). arXiv:hep-ph/9811470
- P. Gambino, P.A. Grassi, Phys. Rev. D **62**, 076002 (2000). <https://doi.org/10.1103/PhysRevD.62.076002>. arXiv:hep-ph/9907254
- P.A. Grassi, B.A. Kniehl, A. Sirlin, Phys. Rev. Lett. **86**, 389 (2001). <https://doi.org/10.1103/PhysRevLett.86.389>. arXiv:hep-th/0005149
- A. Andreassen, W. Frost, M.D. Schwartz, Phys. Rev. D **91**, 016009 (2015). <https://doi.org/10.1103/PhysRevD.91.016009>. arXiv:1408.0287 [hep-ph]
- J. Frohlich, G. Morchio, F. Strocchi, Phys. Lett. **97B**, 249 (1980). [https://doi.org/10.1016/0370-2693\(80\)90594-8](https://doi.org/10.1016/0370-2693(80)90594-8)
- J. Frohlich, G. Morchio, F. Strocchi, Nucl. Phys. B **190**, 553 (1981). [https://doi.org/10.1016/0550-3213\(81\)90448-X](https://doi.org/10.1016/0550-3213(81)90448-X)
- A. Maas, Mod. Phys. Lett. A **30**, 1550135 (2015). <https://doi.org/10.1142/S0217732315501357>. arXiv:1502.02421 [hep-ph]
- A. Maas, Prog. Part. Nucl. Phys. **106**, 132 (2019). <https://doi.org/10.1016/j.ppnp.2019.02.003>. arXiv:1712.04721 [hep-ph]
- A. Maas, P. Törek, Ann. Phys. **397**, 303 (2018). <https://doi.org/10.1016/j.aop.2018.08.018>. arXiv:1804.04453 [hep-lat]
- R. Sondenheimer, Phys. Rev. D **101**, 056006 (2020). <https://doi.org/10.1103/PhysRevD.101.056006>. arXiv:1912.08680 [hep-th]
- K.-I. Kondo, Phys. Lett. B **762**, 219 (2016). <https://doi.org/10.1016/j.physletb.2016.09.026>. arXiv:1606.06194 [hep-th]
- K.-I. Kondo, Eur. Phys. J. C **78**, 577 (2018). <https://doi.org/10.1140/epjc/s10052-018-6051-2>. arXiv:1804.03279 [hep-th]
- D. Binosi, A. Quadri, JHEP **09**, 032 (2019). [https://doi.org/10.1007/JHEP09\(2019\)032](https://doi.org/10.1007/JHEP09(2019)032). arXiv:1904.06692 [hep-ph]
- D. Dudal, D. van Egmond, M. Guimarães, O. Holanda, B. Mintz, L. Palhares, G. Peruzzo, S. Sorella, Phys. Rev. D **100**, 065009 (2019). <https://doi.org/10.1103/PhysRevD.100.065009>. arXiv:1905.10422 [hep-th]
- D. Dudal, D.M. van Egmond, M.S. Guimaraes, O. Holanda, L.F. Palhares, G. Peruzzo, S.P. Sorella, JHEP **02**, 188 (2020a). [https://doi.org/10.1007/JHEP02\(2020\)188](https://doi.org/10.1007/JHEP02(2020)188). arXiv:1912.11390 [hep-th]
- M. Capri, I. Justo, L. Palhares, G. Peruzzo, S. Sorella, Phys. Rev. D **102**, 033003 (2020). <https://doi.org/10.1103/PhysRevD.102.033003>. arXiv:2007.01770 [hep-th]
- G. 't Hooft, M. Veltman, Nucl. Phys. B **153**, 365 (1979). [https://doi.org/10.1016/0550-3213\(79\)90605-9](https://doi.org/10.1016/0550-3213(79)90605-9)
- R. Ellis, G. Zanderighi, JHEP **02**, 002 (2008). <https://doi.org/10.1088/1126-6708/2008/02/002>. arXiv:0712.1851 [hep-ph]
- A. Maas, R. Sondenheimer, Phys. Rev. D (2020). <https://doi.org/10.1103/PhysRevD.102.113001>. arXiv:2009.06671 [hep-ph]
- Work in progress
- J.C. Collins, *Renormalization: An Introduction to Renormalization, The Renormalization Group, and the Operator Product Expansion, Cambridge Monographs on Mathematical Physics*, vol. 26 (Cambridge University Press, Cambridge, 1986). <https://doi.org/10.1017/CBO9780511622656>
- P. Colangelo, A. Khodjamirian, *At The Frontier of Particle Physics: Handbook of QCD (in 3 Volumes)* (World Scientific, 2001), pp. 1495–1576. <https://doi.org/10.1142/4544>
- N. Irges, F. Koutroulis, Nucl. Phys. B **924**, 178 (2017). <https://doi.org/10.1016/j.nuclphysb.2017.09.009>. arXiv:1703.10369 [hep-ph]. [Erratum: Nucl. Phys. B **938**, 957 (2019). <https://doi.org/10.1016/j.nuclphysb.2018.09.025>]
- E.H. Fradkin, S.H. Shenker, Phys. Rev. D **19**, 3682 (1979). <https://doi.org/10.1103/PhysRevD.19.3682>
- J. Greensite, *An Introduction to the Confinement Problem*, vol. 821. Lect. Notes Phys. (2011), pp. 1–211. <https://doi.org/10.1007/978-3-642-14382-3>
- A. Cherman, T. Jacobson, S. Sen, L.G. Yaffe, Phys. Rev. D (2020). <https://doi.org/10.1103/PhysRevD.102.105021>. arXiv:2007.08539 [hep-th]
- R. Oehme, W. Zimmermann, Phys. Rev. D **21**, 471 (1980). <https://doi.org/10.1103/PhysRevD.21.471>
- J.M. Cornwall, Phys. Rev. D **26**, 1453 (1982). <https://doi.org/10.1103/PhysRevD.26.1453>
- D. Zwanziger, Nucl. Phys. B **323**, 513 (1989). [https://doi.org/10.1016/0550-3213\(89\)90122-3](https://doi.org/10.1016/0550-3213(89)90122-3)
- R. Alkofer, L. von Smekal, Phys. Rep. **353**, 281 (2001). [https://doi.org/10.1016/S0370-1573\(01\)00010-2](https://doi.org/10.1016/S0370-1573(01)00010-2). arXiv:hep-ph/0007355
- A. Cucchieri, T. Mendes, A.R. Taurines, Phys. Rev. D **71**, 051902 (2005). <https://doi.org/10.1103/PhysRevD.71.051902>. arXiv:hep-lat/0406020
- P.O. Bowman, U.M. Heller, D.B. Leinweber, M.B. Parappilly, A. Sternbeck, L. von Smekal, A.G. Williams, J.-B. Zhang, Phys. Rev. D **76**, 094505 (2007). <https://doi.org/10.1103/PhysRevD.76.094505>. arXiv:hep-lat/0703022
- A. Cucchieri, T. Mendes, Proceedings, 25th International Symposium on Lattice field theory (Lattice 2007): Regensburg, Germany, July 30–August 4, 2007. PoS LATTICE2007, 297 (2007). <https://doi.org/10.22323/1.042.0297>. arXiv:0710.0412 [hep-lat]

43. A. Aguilar, D. Binosi, J. Papavassiliou, Phys. Rev. D **78**, 025010 (2008). <https://doi.org/10.1103/PhysRevD.78.025010>. arXiv:0802.1870 [hep-ph]
44. D. Dudal, J.A. Gracey, S.P. Sorella, N. Vandersickel, H. Verschelde, Phys. Rev. D **78**, 065047 (2008). <https://doi.org/10.1103/PhysRevD.78.065047>. arXiv:0806.4348 [hep-th]
45. A. Maas, Phys. Rev. D **79**, 014505 (2009). <https://doi.org/10.1103/PhysRevD.79.014505>. arXiv:0808.3047 [hep-lat]
46. C.S. Fischer, A. Maas, J.M. Pawłowski, Ann. Phys. **324**, 2408 (2009). <https://doi.org/10.1016/j.aop.2009.07.009>. arXiv:0810.1987 [hep-ph]
47. D. Binosi, J. Papavassiliou, Phys. Rep. **479**, 1 (2009). <https://doi.org/10.1016/j.physrep.2009.05.001>. arXiv:0909.2536 [hep-ph]
48. I.L. Bogolubsky, E.M. Ilgenfritz, M. Müller-Preussker, A. Sternbeck, Phys. Lett. B **676**, 69 (2009). <https://doi.org/10.1016/j.physletb.2009.04.076>. arXiv:0901.0736 [hep-lat]
49. V.G. Bornyakov, V.K. Mitrjushkin, M. Müller-Preussker, Phys. Rev. D **81**, 054503 (2010). <https://doi.org/10.1103/PhysRevD.81.054503>. arXiv:0912.4475 [hep-lat]
50. A. Cucchieri, T. Mendes, Phys. Rev. D **81**, 016005 (2010). <https://doi.org/10.1103/PhysRevD.81.016005>. arXiv:0904.4033 [hep-lat]
51. M. Tissier, N. Wschebor, Phys. Rev. D **82**, 101701 (2010). <https://doi.org/10.1103/PhysRevD.82.101701>. arXiv:1004.1607 [hep-ph]
52. M. Tissier, N. Wschebor, Phys. Rev. D **84**, 045018 (2011). <https://doi.org/10.1103/PhysRevD.84.045018>. arXiv:1105.2475 [hep-th]
53. P. Boucaud, J.P. Leroy, A.L. Yaouanc, J. Micheli, O. Pene, J. Rodriguez-Quintero, Few Body Syst. **53**, 387 (2012). <https://doi.org/10.1007/s00601-011-0301-2>. arXiv:1109.1936 [hep-ph]
54. J. Serreau, M. Tissier, Phys. Lett. B **712**, 97 (2012). <https://doi.org/10.1016/j.physletb.2012.04.041>. arXiv:1202.3432 [hep-th]
55. O. Oliveira, P.J. Silva, Phys. Rev. D **86**, 114513 (2012). <https://doi.org/10.1103/PhysRevD.86.114513>. arXiv:1207.3029 [hep-lat]
56. J.M. Cornwall, Mod. Phys. Lett. A **28**, 1330035 (2013). <https://doi.org/10.1142/S0217732313300358>. arXiv:1310.7897 [hep-ph]
57. A.C. Aguilar, D. Binosi, J. Papavassiliou, Phys. Rev. D **89**, 085032 (2014). <https://doi.org/10.1103/PhysRevD.89.085032>. arXiv:1401.3631 [hep-ph]
58. M. Peláez, M. Tissier, N. Wschebor, Phys. Rev. D **90**, 065031 (2014). <https://doi.org/10.1103/PhysRevD.90.065031>. arXiv:1407.2005 [hep-th]
59. U. Reinosa, J. Serreau, M. Tissier, N. Wschebor, Phys. Rev. D **91**, 045035 (2015). <https://doi.org/10.1103/PhysRevD.91.045035>. arXiv:1412.5672 [hep-th]
60. F. Siringo, Phys. Rev. D **94**, 114036 (2016). <https://doi.org/10.1103/PhysRevD.94.114036>. arXiv:1605.07357 [hep-ph]
61. A.K. Cyrol, L. Fister, M. Mitter, J.M. Pawłowski, N. Strodthoff, Phys. Rev. D **94**, 054005 (2016). <https://doi.org/10.1103/PhysRevD.94.054005>. arXiv:1605.01856 [hep-ph]
62. A.G. Duarte, O. Oliveira, P.J. Silva, Phys. Rev. D **94**, 014502 (2016). <https://doi.org/10.1103/PhysRevD.94.014502>. arXiv:1605.00594 [hep-lat]
63. U. Reinosa, J. Serreau, M. Tissier, A. Tresmontant, Phys. Rev. D **95**, 045014 (2017). <https://doi.org/10.1103/PhysRevD.95.045014>. arXiv:1606.08012 [hep-th]
64. M. Frasca, Eur. Phys. J. Plus **132**, 38 (2017). <https://doi.org/10.1140/epjp/i2017-11321-4>. arXiv:1509.05292 [math-ph]. [Erratum: Eur. Phys. J. Plus **132**(5), 242 (2017). <https://doi.org/10.1140/epjp/i2017-11563-0>]
65. P. Lowdon, Nucl. Phys. B **935**, 242 (2018). <https://doi.org/10.1016/j.nuclphysb.2018.08.012>. arXiv:1711.07569 [hep-th]
66. G. Comitini, F. Siringo, Phys. Rev. D **97**, 056013 (2018). <https://doi.org/10.1103/PhysRevD.97.056013>. arXiv:1707.06935 [hep-ph]
67. M.Q. Huber, *Nonperturbative Properties of Yang–Mills Theories*, habilitation, Graz U. (2018). arXiv:1808.05227 [hep-ph]
68. Y. Hayashi, K.-I. Kondo, Phys. Rev. D **99**, 074001 (2019). <https://doi.org/10.1103/PhysRevD.99.074001>. arXiv:1812.03116 [hep-th]
69. D. Binosi, R.-A. Tripolt, Phys. Lett. B **801**, 135171 (2020). <https://doi.org/10.1016/j.physletb.2019.135171>. arXiv:1904.08172 [hep-ph]
70. J.A. Gracey, M. Peláez, U. Reinosa, M. Tissier, Phys. Rev. D **100**, 034023 (2019). <https://doi.org/10.1103/PhysRevD.100.034023>. arXiv:1905.07262 [hep-th]
71. K.-I. Kondo, M. Watanabe, Y. Hayashi, R. Matsudo, Y. Suda, Eur. Phys. J. C **80**, 84 (2020). <https://doi.org/10.1140/epjc/s10052-020-7632-4>. arXiv:1902.08894 [hep-th]
72. D. Dudal, O. Oliveira, M. Roelfs, P. Silva, Nucl. Phys. B **952**, 114912 (2020b). <https://doi.org/10.1016/j.nuclphysb.2019.114912>. arXiv:1901.05348 [hep-lat]
73. C.S. Fischer, M.Q. Huber, Phys. Rev. D **102**(9), 094005 (2020). <https://doi.org/10.1103/PhysRevD.102.094005>. arXiv:2007.11505 [hep-ph]
74. M. Capri, D. Dudal, D. Fiorentini, M. Guimaraes, I. Justo, A. Pereira, B. Mintz, L. Palhares, R. Sobreiro, S. Sorella, Phys. Rev. D **92**, 045039 (2015). <https://doi.org/10.1103/PhysRevD.92.045039>. arXiv:1506.06995 [hep-th]
75. M. Capri, D. Dudal, M. Guimaraes, A. Pereira, B. Mintz, L. Palhares, S. Sorella, Phys. Lett. B **781**, 48 (2018). <https://doi.org/10.1016/j.physletb.2018.03.058>. arXiv:1802.04582 [hep-th]
76. M. Lavelle, D. McMullan, Phys. Rep. **279**, 1 (1997). [https://doi.org/10.1016/S0370-1573\(96\)00019-1](https://doi.org/10.1016/S0370-1573(96)00019-1). arXiv:hep-ph/9509344
77. M. Shifman, *Advanced Topics in Quantum Field Theory: A Lecture Course* (Cambridge University Press, Cambridge, 2012)
78. G. Passarino, M.J.G. Veltman, Nucl. Phys. B **160**, 151 (1979). [https://doi.org/10.1016/0550-3213\(79\)90234-7](https://doi.org/10.1016/0550-3213(79)90234-7)